

Reheating in R^2 Palatini inflationary models

Ioannis D. Gialamas^{a*} and A. B. Lahanas^{a†}

^a *National and Kapodistrian University of Athens,
Department of Physics,
Nuclear and Particle Physics Section,
GR-157 71 Athens, Greece*

We consider R^2 inflation in the Palatini gravity assuming the existence of scalar fields, coupled to gravity in the most general manner. These theories, in the Einstein frame, and for one scalar field h , share common features with K - inflation models. We apply this formalism for the study of popular inflationary models, whose potentials are monomials, $V \sim h^n$, with n a positive even integer. We also study the Higgs model non-minimally coupled to gravity. Although these have been recently studied, in the framework of the Palatini approach, we show that the scalar power spectrum severely constrains these models. Although we do not propose a particular reheating mechanism, we show that the quadratic $\sim h^2$ and the Higgs model can survive these constraints with a maximum reheating temperature as large as $\sim 10^{15} GeV$, when reheating is instantaneous. However, this can be only attained at the cost of a delicate fine-tuning of couplings. Deviations from this fine-tuned values can still yield predictions compatible with the cosmological data, for couplings that lie in very tight range, giving lower reheating temperatures.

Keywords: Modified Theories of Gravity, Inflationary Universe

PACS: 04.50.Kd, 98.80.Cq

I. INTRODUCTION

It has been long known that the Palatini formulation of General Relativity (GR), or first-order formalism, is an alternative to the well-known metric formulation, or second-order formalism. In the latter the space time connection is determined by the metric while in the Palatini approach the connection $\Gamma_{\lambda\sigma}^{\mu}$ is treated as an independent variable [1–8], (see also [9], and references therein). It is through the use of the equations of motion that $\Gamma_{\lambda\sigma}^{\mu}$ receive the well known form of the Christoffel symbols, describing thus a metric connection. Within the context of GR the two formulations are equivalent. However in the presence of fields that are coupled in a non-minimal manner to gravity this no longer holds, [1–3]. In that case the two formulations describe different physical theories.

Encompassing the popular inflation models into Palatini Gravity, in an effort to describe the cosmological evolution of the Universe, leads to different cosmological predictions, from the metric formulation, due to the fact that the dynamics of the two approaches differ. A notable example is the Starobinsky model, for instance, where except the graviton there exists an additional propagating scalar degree of freedom, the scalaron, whose mass is related to the coefficient of the R^2 term. In the Einstein frame this shows up as a dynamical scalar field, the inflaton, moving in a potential, the celebrated Starobinsky potential, [10–12]. Within the framework of the Palatini Gravity, in any $f(R)$ theory [3], there are no

*Electronic address: i.gialamas@phys.uoa.gr

†Electronic address: alahanas@phys.uoa.gr

extra propagating degrees of freedom, that can play the role of the inflaton, and hence the inflaton has to be put in by hand as an additional field coupled to $f(R)$ gravity.

The differences between metric and Palatini formulation in the cosmological predictions, as far as inflation is concerned, arise from the non-minimal couplings of the scalars, that take-up the role of the inflaton. These couplings are different in the two approaches. This has been first pointed out in [13] and has attracted the interest of many authors since, [14–42], with still continuing activity, [43–49].

The measurements of the cosmological parameters, by various collaborations, has tighten the allowed limits of these observables which in turn constrain severely, or even exclude, particular inflationary models, [50–52]. In particular, the spectral index n_s and the bounds on the tensor-to-scalar ratio r impose severe restrictions and not all models can be compatible with the observational data ¹. Within the class of $f(R)$ theories the Starobinsky model, which is an R^2 - theory, is singled out, although other popular models can also successfully pass the tests provided by the recent cosmological observations. The measurements of the primordial scalar perturbations, and of the associated power spectrum amplitude A_s , constrains the scale of inflation in models encompassed in the framework of the metric formulation. We shall show that in the Palatini formalism this imposes restrictions that are more stringent, at least in some cases, than the ones arising from the observables n_s, r and should be duly taken into account. In this work we shall consider \mathcal{R}^2 theories, in the framework of the Palatini Gravity, and study the cosmological predictions of some of the popular models existing in literature. We will show that these do not comfortably stand, unless the parameters describing the models are fine-tuned, the main source of this fine-tuning being the power spectrum amplitude.

This paper is organized as follows :

In section II, we present the salient features and give a general setup of $f(\mathcal{R})$ - theory ², in the presence of an arbitrary number of scalar fields, coupled to gravity in a non-minimal manner, in general. Although this is not new, as this effort has been undertaken by other authors as well, we think that the general, and model-independent, expressions we arrive at, are worth being discussed. We shall then focus on the case of \mathcal{R}^2 theories for which the passage to the Einstein frame is easily implemented. These theories have a gravity sector, specified by two arbitrary functions, sourcing in general non-minimal couplings of the scalars involved in Palatini Gravity and a third function which is the scalar potential. In the Einstein frame, and when a single field is present, these models have much in common with the K - inflation models [54].

In section III, we discuss the arising equations of motions and the slow-roll mechanism, and give the pertinent slow-roll parameters, adapted to the particular setup. This is necessary since it is our aim to employ a scheme in which the passage to canonically normalized fields is not mandatory. This we find it more convenient especially because the use of canonically normalized fields results, in most of the cases, to expressions that cannot be cast in closed forms.

The discussion of the cosmological observables is the subject of section IV. We focus, in particular, to the power spectrum amplitude which, as already advertised, puts severe constraints on the inflation models that we are going to discuss. We find it necessary to include higher order corrections, in the slow-roll parameters, of the power spectrum, since these may account for contributions comparable, in magnitude, to the errors associated with the power spectrum. Although we shall not adopt a particular reheating mechanism, the dependence of the number of e-folds on the reheating temperature is of paramount importance, for the study of the cosmological predictions. This is, also, reviewed in section IV.

In section V, we consider particular inflation models, namely the class of models in which the scalar field h , is characterized by monomial potentials $\sim h^n$, with n a positive even integer, and the Higgs model. Although these have been much studied, we shall show that the cosmological data put severe restrictions on the associated couplings leading to fine-tuned adjustments of the parameters involved, when the power spectrum data are taken into account. The reheating mechanism can be instantaneous, at the cost of an unnatural fine-tuning of the couplings pertinent to the potential, describing the aforementioned

¹ In this work, standard assumptions are made for neutrino masses and their effective number. Relaxing these it induces substantial shifts in n_s [53].

² Throughout this paper we use different symbols for the Ricci scalar which in the metric formulation we denote by R , and in the Palatini approach denoted by \mathcal{R} .

models. For the models discussed, the instantaneous reheating temperature T_{ins} , which sets the maximum temperature, can be as large as $\sim 10^{15} GeV$. Departing from these fine-tune values, we can still be in agreement with all data, with temperatures that are significantly lower than the instantaneous reheating temperature. This requires that the coupling of the potential lies within a very tight range. Outside this range these models cannot be made compatible with the power spectrum data for any value of the equation of state parameter w in the range $-1/3 < w < 1$.

In sections VI, we end up with our conclusions.

II. THE MODEL

We shall consider an action where scalar fields h^J are coupled to gravity in the following manner

$$S = \int d^4x \sqrt{-g} \left(f(\mathcal{R}, h) + \frac{1}{2} G_{IJ}(h) \partial h^I \partial h^J - V(h) \right). \quad (1)$$

In it \mathcal{R} is the scalar curvature in the Palatini formalism and $f(\mathcal{R}, h)$ and arbitrary function of the scalars h^J and \mathcal{R} . This action is reminiscent of an $f(R)$ theory in which scalar fields are involved with kinetic terms written in the most general way resembling σ - models. Following standard procedure we write this action in the following manner, introducing the auxiliary field Φ .

$$S = \int d^4x \sqrt{-g} \left(f(\Phi, h) + f'(\Phi, h) (\mathcal{R} - \Phi) + \frac{1}{2} G_{IJ}(h) \partial h^I \partial h^J - V(h) \right). \quad (2)$$

In this $f'(\Phi, h)$ denotes the derivative with respect Φ . One can define ψ in the following way

$$\psi = \frac{\partial f(\Phi, h)}{\partial \Phi}, \quad \text{with inverse} \quad \Phi = \Phi(\psi, h), \quad (3)$$

so the action is written as follows,

$$S = \int d^4x \sqrt{-g} \left(\psi \mathcal{R} + \frac{1}{2} G_{IJ}(h) \partial h^I \partial h^J - \psi \Phi + f(\Phi, h) - V(h) \right). \quad (4)$$

One can go to the Einstein frame by performing a Weyl transformation of the metric

$$g_{\mu\nu} = \lambda \bar{g}_{\mu\nu}, \quad \text{with} \quad \lambda \psi = \frac{1}{2}. \quad (5)$$

That done the theory in the Einstein frame receives the following form,

$$S = \int d^4x \sqrt{-\bar{g}} \left(\frac{\bar{\mathcal{R}}}{2} + \frac{1}{4\psi} G_{IJ}(h) \partial h^I \partial h^J - \frac{1}{4\psi^2} (\psi \Phi - f(\Phi, h) + V(h)) \right). \quad (6)$$

The last step is to eliminate the field ψ whose equation of motion is trivially found to be

$$\psi (\partial h)^2 = \psi \Phi - 2f(\Phi, h) + 2V(h), \quad (7)$$

where, in order to speed up notation, we have denoted $G_{IJ}(h) \partial h^I \partial h^J = (\partial h)^2$.

Note that (7) is not solvable, in general, but we shall exemplify it in \mathcal{R}^2 -theories where this can be analytically solved. In the following we shall focus on such theories which can be considered as generalizations of the Starobinsky action. However there are two major differences, first the coefficients of the linear and quadratic, in the curvature \mathcal{R} , terms are not in general constants, and second the framework is the Palatini formalism in which the connection is not the well-known Christoffel connection but it is treated as an independent field.

We shall apply the previous formalism when only a single scalar, h , is present and $f(h, \mathcal{R})$ is quadratic in the curvature having the form

$$f(\mathcal{R}, h) = \frac{g(h)}{2} \mathcal{R} + \frac{\mathcal{R}^2}{12M^2(h)}. \quad (8)$$

Since a single scalar field is assumed its kinetic term can be always brought to the form $(\partial h)^2/2$, that is in the action (1) the field can be taken canonically normalized. Therefore in this theory there are three arbitrary functions, namely $g(h)$, $M^2(h)$, $V(h)$, and any choice of them specifies a particular model. We have set the reduced Planck mass $m_P = (8\pi G_N)^{-1/2}$ dimensionless and equal to unity and thus all quantities in (8) are dimensionless. When we reinstate dimensions the functions g, V have dimensions $mass^2, mass^4$, respectively, while M^2 is dimensionless. Note that a non-trivial field dependence of the functions $g(h)$ and $/$ or $M^2(h)$ is a manifestation of non-minimal coupling of the scalar h to Palatini Gravity. Note that since we employ Palatini formalism, there is no a scalaron field, associated with an additional propagating degree of freedom, which in the Einstein frame of the metric formulation play the role of the inflaton.

With the function $f(\mathcal{R}, h)$ as given by (8) we get from Eq. (3),

$$\psi = \frac{g(h)}{2} + \frac{\Phi}{6M^2(h)}, \quad (9)$$

whose inverse is,

$$\Phi = 6M^2(h) \left(\psi - \frac{g(h)}{2} \right). \quad (10)$$

Using these we can solve (7) in terms of ψ in a trivial manner,

$$\psi = \frac{4V + 3M^2g^2}{2(\partial h)^2 + 6M^2g}, \quad (11)$$

that is ψ , and hence Φ from (10), are expressed in terms of $h, (\partial h)^2$. Plugging ψ, Φ into (6) we get, in a straightforward manner,

$$S = \int d^4x \sqrt{-g} \left(\frac{\mathcal{R}}{2} + \frac{K(h)}{2} (\partial h)^2 + \frac{L(h)}{4} (\partial h)^4 - V_{eff}(h) \right). \quad (12)$$

In this action we have suppressed the bar in the the scalar curvature and, also, $\sqrt{-g}$, and in order to simplify notation we have denoted $\partial_\mu h \partial^\mu h$ by $(\partial h)^2$ and $(\partial_\mu h \partial^\mu h)^2$ by $(\partial h)^4$. Note the appearance of quartic terms $(\partial h)^4$ in the action. As for the functions K, L, V_{eff} , appearing in (12), they are analytically given by

$$L(h) = (3M^2g^2 + 4V)^{-1}, \quad K(h) = 3M^2gL, \quad V_{eff} = 3M^2VL. \quad (13)$$

Observe that since terms up to \mathcal{R}^2 have been considered, in the $f(\mathcal{R})$ - gravity, higher than $(\partial h)^4$ terms do not appear in the action.

The above Lagrangean may feature, under conditions, K - inflation models [54], which involve a single field, described by an action whose general form is

$$S = \int \sqrt{-g} \left(\frac{\mathcal{R}}{2} + p(h, X) \right) d^4x. \quad (14)$$

where $X \equiv (1/2)\partial_\mu h \partial^\mu h$. The comological perturbations of such models were considered in [55]. However the importance of a time-dependend speed of sound c_s in K - inflations models was emphasized in [56] and cosmological constraints were derived, using improved expressions for the density perturbations power spectra. Specific models with $p(h, X) = F(X) - V(h)$ were considered in [57]. In (12) the Lagrangean

density involving the scalar field is identified with $p(h, X)$, but the function $F(X)$ is now replaced by $K(h)X + L(h)X^2$, which depends, in addition to X , on the field h , as well, through $K(h), L(h)$.

In a flat Robertson-Walker metric, where the background field h is only time dependent, the energy density and pressure are given by

$$\rho(h, X) = K(h)X + 3L(h)X^2 + V_{eff}(h) \quad , \quad p(h, X) = K(h)X + L(h)X^2 - V_{eff}(h), \quad (15)$$

with X being, in this case, half of the velocity squared, $X = \dot{h}^2/2$.

We shall assume that the function $L(h)$ is always positive to avoid phantoms, which may lead to an equation of state with $w < -1$. This may occur when $L < 0$ and X becomes sufficiently large. However, there is no restriction for the sign of $K(h)$ which may be negative in some regions of the field space, signaling that the kinetic term has the wrong sign in those regions. Obviously the sign of $K(h)$ should be positive at the minimum of the potential. Options where K is negative in some regions, although interesting, will not be pursued in this work. Besides, we shall assume that the potential is positive $V_{eff}(h) \geq 0$ and it has a Minkowski vacuum. This ensures that the energy density is positive definite. When inflation models are considered, the inflaton will roll down towards this minimum signaling the end of inflation and beginning of Universe thermalization. These are rather mild conditions.

Concerning the potential V_{eff} , appearing in the Lagrangian (12) in the Einstein frame, from the last of (13) we see that due to the fact that we have assumed $L, M^2 > 0$, positivity of $V_{eff} \geq 0$ entails $V \geq 0$. Moreover one can trivially show, from (13), that V_{eff} be cast in the following form,

$$V_{eff} = \frac{3M^2}{4} \left(1 - \frac{K^2}{3M^2L} \right). \quad (16)$$

From this it is seen that besides being positive the potential is bounded from above by,

$$V_{eff} \leq \frac{3M^2}{4}. \quad (17)$$

This upper bound can be easily saturated, for large h , by choosing appropriately the functions involved, namely g, M^2 and V . Actually the asymptotic values of these functions, for large h , control the behavior of the potential in this regime³. If we opt that the function M^2 approaches a plateau, or is constant, so does the potential which may therefore drive successful inflation. The requirement to have a Minkowski vacuum can be, also, easily satisfied, and therefore many options are available for potentials bearing the characteristics demanded for the inflationary slow-roll mechanism to be implemented. This will be exemplified in specific models, to be discussed later.

Concluding this section, we presented a general, and model independent, framework of \mathcal{R}^2 - theories, in the Palatini formulation of Gravity, which may be useful for the study of inflation models and may support slow-roll inflation. In the Einstein frame these theories have much in common with the K -inflation models. This formalism will be implemented, for the study of various models of inflation in the following sections.

III. THE EQUATIONS OF MOTION AND THE SLOW-ROLL

When non canonical kinetic terms are present the equations of motions for the would be inflaton scalar field h differ from their standard form. As a result, the cosmological parameters describing the slow-roll evolution should be modified appropriately. Certainly one can normalize the kinetic term of the scalar field appropriately but this is not always very convenient. Actually the integrations needed, in order to

³ It is fairly easy to see that saturation of the bound (17), for large field values, is easily obtained if $\frac{g^2}{V} \rightarrow 0$, and $\frac{g^2 M^2}{V} \ll 1$, as $h \rightarrow large$.

pass from the non canonical to the canonical field, are not easy, in most of the cases, to be carried and the results cannot be presented in a closed form. Therefore it proves easier to work directly with the non canonical fields and express the pertinent cosmological observables in a manner that is appropriate for this treatment.

It is not hard to see that the field h satisfies the equation of motion given by

$$(K + 3L \dot{h}^2)\ddot{h} + 3H(K + L \dot{h}^2)\dot{h} + V'_{eff}(h) + \frac{1}{4}(2K' + 3L' \dot{h}^2)\dot{h}^2 = 0, \quad (18)$$

in it all primes denote derivatives with respect h . If the field were canonical, $K = 1$, and there were no quartic in the velocity terms, that is $L = 0$, then the equation above receives its well-known form. In this, the effect of using a non canonical, in general, field h is encoded in the function K . The effect of the presence of terms $(\partial h)^4$ in the action is encoded within the function L . The terms that depend on L are multiplied by an extra power of the velocity squared, as compared to the K -terms. These cannot be neglected although, as we discuss below, they are small in particular models, during inflation.

We can gain more insight is we momentarily use a canonically normalized field, say ϕ , defined by

$$\phi = \int \sqrt{K(h)} dh. \quad (19)$$

To avoid ghosts we shall assume that $K > 0$, so that the integration above makes sense. Actually if K is negative the kinetic term of the field ϕ will have the wrong sign, i.e. $-(\partial\phi)^2/2$. It could happen however that this function is negative in some region but at the Minkowski vacuum is strictly positive. In this way ghosts are also avoided. This case, interesting as might be, is not discussed and we prefer to take a rather conservative view point of having $K > 0$ in the whole region. Then in terms of the field ϕ the equation of motion (18) takes up the form

$$\left(1 + \frac{3L}{K^2}\dot{\phi}^2\right)\ddot{\phi} + 3H\left(1 + \frac{L}{K^2}\dot{\phi}^2\right)\dot{\phi} + \frac{dV_{eff}}{d\phi} + \frac{3L}{4K^2}\frac{d\ln(L/K^2)}{d\phi}\dot{\phi}^4 = 0. \quad (20)$$

From this form it appears that the smallness of the ∂h^4 terms in the action is quantified by the smallness of the ratio $\frac{L}{K^2}\dot{\phi}^2 \ll 1$, which is equivalent to $\frac{L}{K}\dot{h}^2 \ll 1$. Neglecting this in the equation above we recover the well-known form of the equation of motion for the canonical field ϕ .

However, it should be stressed that our numerical study duly takes into account the contribution of these terms and no approximation, whatsoever, is made, although we have found numerically that they are small, at least in the models under consideration in this work. This has been also pointed out in [31–33, 38]. In order to show this, and anticipating conclusions based on our numerical treatment that are presented in forthcoming sections, in Figure 1 we plot on the left panel the evolution of the field h versus the number of e-folds $N = \ln(a_{end}/a(t))$, from the time the number of e-folds reached $N = 70$ to the end of inflation corresponding to $N = 0$. On the right panel, we display the parameter $\epsilon_1 = -\frac{\dot{H}}{H^2}$, the sound of speed squared c_s^2 and the evolution of $\frac{L}{K}\dot{h}^2$. For reference, we have also included a vertical band to mark the region $N = 50 - 60$, usually quoted in literature. These plots regard the minimally coupled model, for which $g = 1$, $M^2 = \frac{1}{3a}$ and $V = \frac{m^2}{2}h^2$. The values of the parameters a, m^2 , used in producing Figure 1, correspond to Model I (C - case), discussed later in section V. for which $a = 2.0 \times 10^9$ and $m = 6.32 \times 10^{-6}$. However similar findings hold for the other models studied in this work, as well.

On the left pane of this figure one notices the rapid damped oscillations of h , after the end of inflation, when it starts falling to the minimum of the potential. These are clearly visible in the magnified inserted small figure. From the right pane, one can see that $\epsilon_1 \ll 1.0$, $c_s^2 \simeq 1.0$, and $\frac{L}{K}\dot{h}^2 \sim \mathcal{O}(10^{-2})$, for any number of e-folds that is larger than about 5, or even smaller. For $N \lesssim 5$ the function ϵ_1 starts growing and $\frac{L}{K}\dot{h}^2$ increases significantly, however its magnitude stays small till the end of inflation.

On the other hand, the scales of interest, from CMB observations, are within the range $10^{-4}Mpc^{-1} \lesssim k \lesssim 10^{-1}Mpc^{-1}$ and the number of e-folds that are left to the end of inflation, from time t_k a scale k crossed the sound horizon, is $N_k = \ln(a_{end}/a(t_k))$. Even for the largest scale, in the aforementioned range, the number of e-folds cannot be less than about $\simeq 20$, as we have found numerically. Therefore, any scale k in the range of interest, crossed the sound horizon long before the end of inflation, when

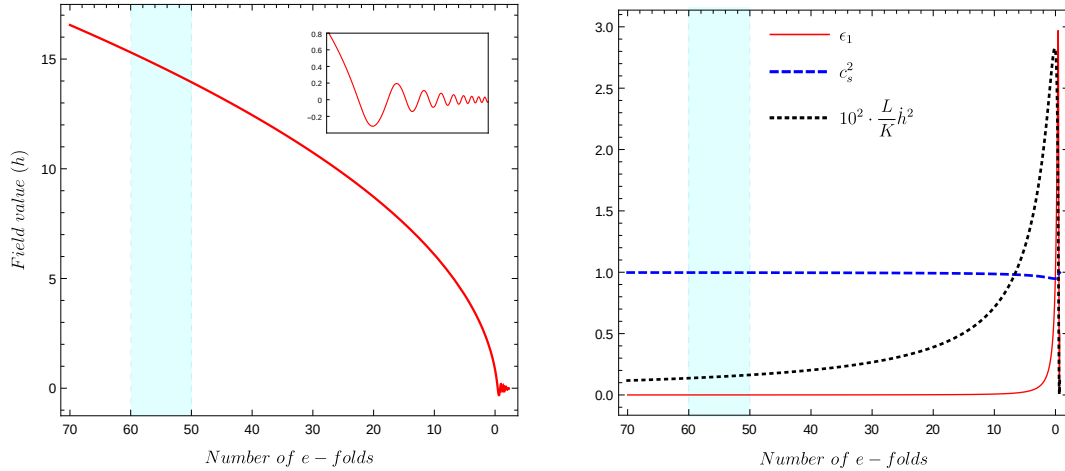


FIG. 1: On the left pane the evolution of the field h with number of e-folds is shown. In the small inset figure, the rapid oscillations of h , as it approaches the minimum of the potential, are shown magnified. On the right we display the parameter ϵ_1 , the sound speed squared c_s^2 and the quantity $10^2 L \dot{h}^2 / K$.

$\epsilon_1 \ll 1.0$, $c_s^2 \simeq 1.0$, and $\frac{L}{K} \dot{h}^2$ was small $\mathcal{O}(10^{-2})$. Therefore, for the cosmological scales of interest the contribution of the L - terms is small.

Although small, for a broad range of the parameters and for the class of models studied here, the role of $\frac{L}{K} \dot{h}^2$ is important in the determination of the energy density ρ_{end} at the end of inflation, which in turn affects the instantaneous reheating temperature T_{ins} . This delicate issue will be discussed later in Section V. Even in this case, however, we have found that the values of ρ_{end} deviate from those obtained approximately by factors of order $\mathcal{O}(1)$.

The previous arguments state that, for the cases of interest to us, one can use the slow-roll approximation and at the same time neglect the L - terms, provided their omission is adequately justified. We repeat that, our results are based on a numerical study and no such an approximation is made. However, this does not deprive us from the right, and for an analytic treatment of the models under consideration, to present qualitative arguments, based on this approximate scheme, aiming at a better understanding of the results that are reached based on a numerical study in which all terms are included and no approximation is made.

Provided that the contribution of the L - term is small, and with $K > 0$, the first slow-roll parameters, as defined in terms of the potential are given by, in terms of the non canonical field h ,

$$\epsilon_V = \frac{1}{2K(h)} \left(\frac{V'_{eff}}{V_{eff}} \right)^2, \quad \eta_V = \frac{\left(K^{-1/2} V'_{eff} \right)'}{K^{1/2} V_{eff}}. \quad (21)$$

In these equations primes denote derivatives with respect the field h . It is trivial to show that these definitions indeed coincide with the well-known definitions if the canonically normalized field ϕ of Eq. (19), is used. As for the the number of e-folds, left to the end of inflation, this is given by

$$N_* = \int_{h_{end}}^{h_*} K(h) \frac{V_{eff}(h)}{V'_{eff}(h)} dh. \quad (22)$$

In this h_* is the pivot value and h_{end} the value of the field at the end of inflation.

IV. COSMOLOGICAL OBSERVABLES

Concerning the cosmological observables, we start by discussing the scalar and tensor power spectra which play an important role in inflationary cosmology. The CMB observations restrict considerably the predictions of inflationary models, in general, and also put severe constraints on specific models, encompassed in the framework of the Palatini Gravity, as we shall analyze in forthcoming sections.

There is a long history on studies towards this direction the first calculations were performed in [58–60]. Since then there has been an intense activity in the field using different methods and improvement of the calculations, by considering higher order corrections, demanded by the precise measurements of the cosmological parameters, or tackle theories with a variable speed of sound, [56, 61–77]

Choosing an arbitrary pivot scale, k^* , that exited the sound horizon at t^* , that is $k^*c_s(t^*) = a(t^*)H(t^*)$, the scalar and tensor power spectra can be expanded about this pivot. keeping the first order terms in the slow-roll parameters, one has

$$\mathcal{P}_\zeta(k) = \frac{H_*^2}{8\pi^2 m_p^2 \epsilon_1^* c_s^*} A \left(1 - 2(D+1)\epsilon_1^* - D\epsilon_2^* - (2+D)s_1^* + (-2\epsilon_1^* - \epsilon_2^* - s_1^*) \ln \frac{k}{k^*} \right) \quad (23)$$

and

$$\mathcal{P}_h(k) = \frac{2H_*^2}{\pi^2 m_p^2} A \left(1 - 2(D+1 - \ln c_s^*)\epsilon_1^* + (-2\epsilon_1^*) \ln \frac{k}{k^*} \right) \quad (24)$$

A subtle point concerns the dependence of the tensor power spectrum on the sound velocity c_s . Usually this is calculated evaluating all quantities at the time of Hubble horizon, which differs, in general, from the time of sound horizon. However if we want to compare the scalar and tensor spectra using the results of cosmological measurements the same pivot should be used, for consistency, as has been emphasized in [56, 74–76]. Using a pivot scale $k^*c_s(t^*) = a(t^*)H(t^*)$ in the scalar spectrum a dependence on c_s emerges in the tensor spectrum, as well.

In these equations the Hubble flow functions (HFF), usually referred to as slow-roll parameters, are defined in the usual manner, in terms of the Hubble rate,

$$\epsilon_1 \equiv -\frac{d \ln H}{dN} = -\frac{\dot{H}}{H^2} \quad , \quad \epsilon_2 \equiv \frac{d \ln \epsilon_1}{dN} = \frac{\dot{\epsilon}_1}{\epsilon_1 H} \quad , \quad s_1 \equiv \frac{d \ln c_s}{dN} = \frac{\dot{c}_s}{c_s H} \quad ,$$

where $dN = H dt$. A star in the HFF in the expressions above means that these are evaluated at t^* . The equations (23,24) can be found in references [56, 73, 75, 76]. In those references a slightly different pivot scale is usually quoted, $k_\diamond c_{s\diamond}(\eta_\diamond) = -1/\eta_\diamond$, where η_\diamond is the conformal time, and the corresponding expressions are given in terms of k_\diamond . However to first order, in HFF, they have the same form when the quantities denoted by a diamond symbol are replaced by the corresponding starred ones. It is only the second order terms that are affected and the corresponding coefficients differ. Note that higher order corrections have been calculated but here we retain the next to leading corrections, that is first order in the slow-roll parameters. In [75] the constants A, D are analytically given. In fact their values are $A = 18e^{-3}$ and $D = 1/3 - \ln 3$, as they follow using the *uniform approximation*, a method that is suitable for theories with varying speed of sound c_s , which resembles the WKB method. Taking next order corrections in the adiabatic approximation these constants are dressed (renormalized) and A turns out to be very close to unity while D becomes $D = 7/19 - \ln 3$. For our numerical treatment we shall therefore use the renormalized values. For details we point the reader to reference [75] where a detailed study is presented, encompassing also higher order corrections, and comparison with other calculations is made.

The corresponding amplitudes, for scalar and tensor perturbations, are then given by,

$$A_s(k^*) = \mathcal{P}_\zeta(k^*) \quad , \quad A_t(k^*) = \mathcal{P}_h(k^*) \quad . \quad (25)$$

Concerning the spectral index of the scalar power spectrum, following standard definitions, this is given by

$$n_s = 1 - 2\epsilon_1^* - \epsilon_2^* - s_1^* \quad (26)$$

while the tensor-to- scalar ratio is given by,

$$r \equiv \frac{\mathcal{P}_h(k^*)}{\mathcal{P}_\zeta(k^*)} = 16 \epsilon_1^* c_s^* (1 + 2 \ln c_s^* \epsilon_1^* + D \epsilon_2^* + (2 + D) s_1^*) \quad , \quad (27)$$

to the same order of approximation.

As for the number of e-folds left, $N_k = \ln \frac{a_{end}}{a(t)}$, from the time t some scale k crossed the sound horizon to the end of inflation, this is given by,

$$\begin{aligned} N_k = & \ln \left[\left(\frac{\pi^2}{30} \right)^{\frac{1}{4}} \frac{(g_s^{*,0})^{\frac{1}{3}} T_0}{\sqrt{3} H_0} \right] - \ln \left(\frac{k}{a_0 H_0} \right) - \ln c_s + \frac{1}{4} \left(\ln \frac{3H^2}{m_P^2} + \ln \frac{3H^2 m_P^2}{\rho_{end}} \right) \\ & + \frac{1 - 3w}{12(1+w)} \ln \frac{\rho_{reh}}{\rho_{end}} - \frac{1}{12} \ln g_s^{*(reh)} + \frac{1}{4} \ln \left(\frac{g^{*(reh)}}{g_s^{*(reh)}} \right) . \end{aligned} \quad (28)$$

The Hubble rate, as well as c_s on the right hand side of it, are evaluated at the crossing time t . See [78, 79], and also [80, 81]. Note that, a $-\ln c_s$ is included in the expression for N_k , due to the fact that the speed of sound may not be unity, as is the case in K -inflation models. All other terms are well-known. In this equation g^*, g_s^* are the energy density and entropy density degrees of freedom. In all quantities superscripts or subscripts labeled by 0 or *reh* denote evaluations at present epoch and end of reheating respectively. In this the parameter w is the effective equation of state parameter in reheating period. The last line depends on the reheating values. The first term in the equation for N_k , takes the well-known value 66.89 when the reduced Hubble constant h equals to $h = 0.676$. In the expression above we prefer to present it analytically as in [81]. Taking a different value for h , always within observational limits, the first term will be replaced by $66.89 - \ln(h/0.676)$. Concerning the last term, this is very small and can be omitted, due to the fact that entropy and energy degrees of freedom are very close to each other for temperatures $T > 500 \text{ keV}$. Therefore we shall drop it in the discussion that follows. The term before the last is also small but we shall retain it. In fact assuming the SM content this takes values $g_s^{*(reh)} = 106.75$, for temperatures above $\sim 1 \text{ TeV}$, being smaller for lower temperatures. Therefore this term contributes little, less than $\mathcal{O}(1\%)$. The term, $\sim \ln(3H^2 m_P^2 / \rho_{end})$, is also not expected to be large. The largest contributions stem from the term $\sim \ln(3H^2 / m_P^2)$ and the reheating term, in most of the models, in which the speed of sound is unity. With varying speed of sound the contribution from the $-\ln c_s$ term is positive and may also give significant contribution, in general. The constant w characterizes an effective equation of state parameter. In the following, whenever the pivot scale k^* is used in (28), N_k shall be denoted by N_* .

Given an inflationary model, the largest uncertainties in N_k are mainly due to the period of Universe reheat after this exited from inflation. For a review see for instance [82]. For the scales of interest, these uncertainties yield values of N_k in the range 50 – 60, usually quoted in the literature. The reheating temperature the Universe reached after its thermalization has been extensively studied and various mechanisms and models have been put under theoretical scrutiny, [80–91]. The number of e-folds accrued during the reheating period, ΔN_{reh} , is given by

$$\Delta N_{reh} \equiv \ln \frac{a_{reh}}{a_{end}} = -\frac{1}{3(1+w)} \ln \frac{\rho_{reh}}{\rho_{end}} . \quad (29)$$

The subscripts (reh), (end) in the cosmic scale factor and the energy densities denote that these quantities are evaluated at the end of the reheating period and inflation respectively. The effective equation of state parameter w in the reheating period we consider as a free parameter. At the end of inflation $w = -1/3$ while the value $w = 1/3$ corresponds to the onset of radiation dominance. In the canonical reheating scenario $w = 0$, but values in the range $\simeq 0.0 - 0.25$, or larger, right after inflation, are also possible in some models [81, 92].

For any model given a value of N_k , we have a prediction of ΔN_{reh} and in this sense (28) serves as a probe of the reheating process. Inversely, given a reheating mechanism, within the context of any

particular inflationary model, the value of ΔN_{reh} is fixed, and hence N_* is predicted. In terms of ΔN_{reh} , for given w , one has for the reheating temperature, see for instance [88],

$$T_{reh} = \left(\frac{30}{\pi^2} \frac{\rho_{end}}{g^{*(reh)}} \right)^{1/4} \exp \left(-\frac{3(1+w)\Delta N_{reh}}{4} \right). \quad (30)$$

In our numerical studies we shall adopt the common values $g^{*(reh)} = g_s^{*(reh)} = 106.75$, corresponding to the SM content, as discussed before, for temperatures above $\sim 1 TeV$.⁴ Note that since $a_{reh} > a_{end}$ we have that $\Delta N_{reh} \geq 0$, and therefore due to $w > -1$ the reheating temperature T_{reh} is bounded from above

$$T_{reh} \leq \left(\frac{30}{\pi^2} \frac{\rho_{end}}{g^{*(reh)}} \right)^{1/4}. \quad (31)$$

The bound on the right hand side of this defines the instantaneous reheating temperature, T_{ins} . The temperature T_{reh} reaches this upper bound when the reheating process is instantaneous, in which case $\Delta N_{reh} = 0$. Note that for rapid thermalization we have $\rho_{end} = \rho_{reh}$, from Eq. (29). The reheating temperature should be larger than $\sim 1 MeV$ so that Big Bang Nucleosynthesis (BBN) is not upset. Lower values on T_{reh} have been established in [93] and recently in [94].

In terms of the reheating temperature the number of e-folds N_* , corresponding to a pivot scale say k^* , is written as

$$\begin{aligned} N_* = & 66.89 - \ln c_s^* - \ln \left(\frac{k^*}{a_0 H_0} \right) + \frac{1}{4} \left(\ln \frac{3H_*^2}{m_P^2} + \ln \frac{3H_*^2 m_P^2}{\rho_{end}} \right) - \frac{1}{12} \ln g_s^{*(reh)} \\ & + \frac{1-3w}{3(1+w)} \left(\ln \frac{T_{reh}}{m_P} - \frac{1}{4} \ln \frac{\rho_{end}}{m_P^4} - \frac{1}{4} \ln \frac{30}{\pi^2} + \frac{\ln g^{*(reh)}}{4} \right). \end{aligned} \quad (32)$$

which we shall use in the following. On the right hand side of it H_*, c_s^* are the Hubble rate and the speed of sound are, respectively, evaluated at t^* , the time of sound horizon crossing of the mode k^* . In this we have taken $h = 0.676$. Uncertainties in the value of h little affect N_* , and for this reason we have also dropped the dependence of N_* on $\ln(h/0.676)$.

The appearance of the sound of speed parameter c_s is due to the fact that in the Palatini formulation of \mathcal{R}^2 gravity higher in the velocity \dot{h} terms unavoidably appear, and its value deviates from unity. In fact c_s is defined by

$$c_s^2 = \frac{\partial p / \partial X}{\partial \rho / \partial X}, \quad (33)$$

where X , defined after Eq. (14), is half the velocity squared. In terms of the field h and its velocity \dot{h} this receives the form

$$c_s^2 = \frac{1 + L \dot{h}^2 / K}{1 + 3L \dot{h}^2 / K}. \quad (34)$$

c_s is controlled by $L \dot{h}^2 / K$, the same combination that appears in the equation of motion for the field h , and approaches unity when $L \dot{h}^2 / K \ll 1$.

The Planck 2018 data [50, 51], yield a value for A_s

$$\text{Log}(10^{10} A_s) \simeq 3.04, \quad (35)$$

⁴ With $g^{*(reh)} = 100$ Eq. (30) coincides with that given in [88].

at a pivot scale $k^* = 0.05 Mpc^{-1}$. In slow-roll inflation, in models with $c_s = 1$, this pivot crossed the horizon at times t^* that are well within the slow-roll regime. Then to lowest order in HFF the scalar amplitude of (25) is written as,

$$A_s \simeq \frac{1}{24\pi^2 m_P^4} \frac{V_{eff}^*}{\epsilon_1^*}, \quad (36)$$

Then in this approximation, and using (35), we get

$$\frac{V_{eff}^*}{m_P^4} = 4.97 \times 10^{-7} \epsilon_1^*. \quad (37)$$

The corresponding amplitude for the tensor perturbations, in leading order, is found to be

$$A_t \simeq \frac{2V_{eff}^*}{3\pi^2 m_P^4}, \quad (38)$$

resulting to a tensor to scalar ratio

$$r = \frac{A_t}{A_s} = 16 \epsilon_1^*, \quad (39)$$

which yields, on account of (36)

$$\frac{V_{eff}^*}{m_P^4} = \frac{3\pi^2}{2} A_s r, \quad (40)$$

a well-known result. The Planck 2018 data, when combined with the BICEP2/Keck Array BK15 data, see [51, 52], yield an upper bound $r < 0.063$, which when the pivot scale $k^* = 0.002 Mpc^{-1}$ is used, decreases to $r_{0.002} < 0.058$. With $r < 0.063$ we have an upper bound on the value of the potential given by

$$\frac{V_{eff}^*}{m_P^4} \lesssim 2.0 \times 10^{-9}, \quad (41)$$

which constrains the scale of inflation. In terms of the Hubble rate this is actually the bound $H_*/m_p < 2.5 \times 10^{-5}$ quoted in [50, 51].

The bound $r < 0.063$ translates to a bound on ϵ_1^* , which is actually follows from (39), given by

$$\epsilon_1^* < 0.004. \quad (42)$$

In models with varying speed of sound c_s the previous arguments do not hold, in general, and the role of c_s has to be taken duly into account. This is done in our numerical analysis which will be presented later on. However, as already discussed in the previous section, we have found numerically that c_s is constant and very close to unity for times until the time t^* of the horizon crossing and only at the late stages of inflation deviation of c_s from unity starts to show up. Therefore on these grounds the arguments given before can be used to have a first estimate of the bounds put in the parameters of the models that we will study in the forthcoming sections. However, our final results do not rely on these qualitative arguments but rather on a numerical study where the dependence on c_s is duly considered. Note that separate lower bounds on c_s are obtained from absence of non gaussianities, which are however satisfied in all models considered in this work, due to the fact that c_s^* is very close to unity, as we have already remarked.

V. MODELS

Before embarking on considering specific models and presenting our results, we find it appropriate to briefly outline the procedure followed in this section. As already stated, towards the end of section III,

our predictions are based on a study which solves Friedmann equations and the evolution equation (18) numerically with no-approximations made. However before doing that we find it useful to first employ the slow-roll approximation, neglecting the contribution of L - terms. This is made for comparison with the numerical results which are the only reliable source to reach physics conclusions. In the models under consideration in this work, the numerical study reveals that this approximate scheme makes sense since it is justified by the results of the numerical treatment. It is for this reason it explains at a very satisfactory level the results that are derived by our numerical treatment. However it should be remarked that this may not be a generic feature and may not be valid for other models encompassed within the framework of the Palatini \mathcal{R}^2 Gravity.

Concerning our numerical analysis, the approximate scheme employed is also useful towards having a first estimate of the magnitudes of the parameters involved, which are consistent with the limits imposed by the measurements of the cosmological parameters. In our numerical approach we scan the parameter space starting from initial values of the parameters that fall within the range suggested by this analysis.

In our procedure the time corresponding to the end of inflation, t_{end} , is determined, as usual, by the condition $\epsilon_1(t_{end}) = 1$, or same $\ddot{a}(t_{end}) = 0$. The time t^* , corresponding to the sound horizon crossing, for a chosen pivot scale k^* , for any given reheating temperature T_{reh} , and effective equation of state parameter w , is then found by solving Eq. (32). This is a fairly easy task to implement numerically. That done all quantities at t^* , which refer to the pivot scale k^* , are easily calculated.

A. Minimally coupled models with potentials $\sim h^n$

In this section we consider specific models using the formalism presented in previous sections, and discuss their predictions. An interesting class of models is the one in which the potential V is a monomial in the field h , $V \sim h^n$, with n even integer, and g, M^2 are constants, that is the scalar h couples to gravity in a minimal manner. We set $g = 1$ ⁵ and hence these models are described by

$$g(h) = 1 \quad , \quad M^2(h) = \frac{1}{3a} \quad , \quad V(h) = \frac{\lambda}{n} h^n \quad \text{with } n = \text{positive even integer} \quad . \quad (43)$$

Therefore two parameters, a and λ are involved which are in principle unknown. Cosmological data will constrain their allowed values as we shall see shortly. In order to facilitate the analysis we define the parameter c defined by the combination,

$$c = \frac{4\lambda a}{n} \quad . \quad (44)$$

Then the functions K, L are given by

$$K(h) = (1 + ch^n)^{-1} \quad , \quad L(h) = a(1 + ch^n)^{-1} \quad , \quad (45)$$

while the potential V_{eff} receives the form

$$V_{eff}(h) = \frac{1}{4a} \frac{ch^n}{1 + ch^n} \quad . \quad (46)$$

For large values of h this is $\simeq 1/4a$ therefore $1/a$, which is proportional to M^2 , sets actually the inflation scale.

In order to find the region of the parameters a, λ , or equivalently a, c , which are consistent with cosmological data, we shall first consider the amplitude of the power spectrum A_s . It suffices, for this purpose, to consider the simplified form given by (36), take $c_s^* \simeq 1$ and replace ϵ_1^* by ϵ_V as given by (21).

⁵ When Planck mass is reinstated in the action this corresponds to $g = m_P^2$.

Then from the analytic form of the potential, given before, and from (21) the amplitude A_s of Eq. (36) takes the form, putting $m_P = 1$,

$$A_s \simeq \frac{1}{24\pi^2} \frac{1}{2n^2} \left(\frac{c}{a}\right) h_*^{n+2} = \frac{1}{12\pi^2} \frac{\lambda}{n^3} h_*^{n+2}, \quad (47)$$

where h_* is the value of the field at t^* . One sees immediately that it is the ratio c/a , or equivalently the parameter λ , that controls the magnitude of the amplitude A_s . For the central value of A_s , which is $A_s \simeq 2.1 \times 10^{-9}$, on account of (47), we have

$$\lambda h_*^{n+2} \simeq (2.49 \times 10^{-7}) n^3 \quad \text{or} \quad \left(\frac{c}{a}\right) h_*^{n+2} \simeq (9.95 \times 10^{-7}) n^2. \quad (48)$$

To further quantify the allowed range of the parameters we also need have an estimate for h_* . To this goal we use (22) from which it follows that

$$N_* = \frac{1}{2n} (h_*^2 - h_{end}^2), \quad (49)$$

which yields

$$h_*^2 = 2nN_* + h_{end}^2. \quad (50)$$

h_{end} is defined as the value for which $\epsilon_V = 1$. For the specific models

$$\epsilon_V = \frac{n^2}{2} \frac{1}{h^2(1 + ch^n)}, \quad (51)$$

therefore h_{end}^2 is solution of the equation

$$ch_{end}^{n+2} + h_{end}^2 - \frac{n^2}{2} = 0. \quad (52)$$

For $c = 0$ the solution is exactly $h_{end}^2 = n^2/2$ while for any $c > 0$ the only real and positive solution for h_{end}^2 is easily found to be bounded by $n^2/2$. From this bound on h_{end}^2 and using the fact that N_* is ~ 50 , or so, it follows from (50) that h_* is well approximated by

$$h_* = \sqrt{2nN_*}, \quad (53)$$

provided that $n \ll 4N_*$. This covers a large class of models ranging from $n = 2$ up to $n = 10$ or even larger. Using h_* , given above, A_s of Eq. (47) is written, in terms of N_* , as

$$A_s \simeq \frac{1}{12\pi^2} \frac{\lambda}{n^3} (2nN_*)^{(n/2+1)}. \quad (54)$$

For $A_s \simeq 2.1 \times 10^{-9}$ we have that the coupling λ is constrained to be

$$\lambda \simeq (4.97 \times 10^{-7}) \frac{k^2}{(4k)^k} \frac{1}{N_*^{k+1}} \quad \text{where } n = 2k. \quad (55)$$

Note that this is inverse proportional to N_*^{k+1} . For $N_* = 55$ and for $n = 2$, that is $V \sim h^2$, this yields $\lambda \simeq 4.11 \times 10^{-11}$ while for $k = 2$, that is $V \sim h^4$ we get $\lambda \simeq 1.87 \times 10^{-13}$. Note that for the $n = 4$ case Eq. (54) coincides with that given in [38]. In that work a small value of the quartic coupling, $\lambda \simeq 2.0 \times 10^{-13}$, is also quoted, quite close to ours given before.

As for the parameter a a lower bound can be established from the bound (41), that is from the observational bound on the tensor to scalar ratio r . Using the analytic form of the potential one finds

$$\frac{1}{4a} \frac{ch_*^n}{1 + ch_*^n} < 2.0 \times 10^{-9}. \quad (56)$$

Replacing c in terms of a from (44), and using the value of h_* given before in (53), we have from (56), after some trivial manipulations,

$$a \gtrsim 10^8 \left(1.25 - \frac{N_*}{50n} \right). \quad (57)$$

For instance, for the quartic potential $V \sim h^4$ and for $N_* = 55$ this yields $a \geq 0.97 \times 10^8$, resulting to an inflationary scale, lower than $\sim 10^{-5}$, or so. Note that (57) is the lowest allowed value of a consistent with the power spectrum and the bound on the potential imposed by the tensor to scalar ratio $r < 0.063$.

The constraints on the parameters given before arise from the amplitude of the power spectrum, in combination with the bound on r , and set the range where acceptable values for A_s can be obtained, However the primordial tilt n_s puts additional constraints and in order to have an estimate of it we use the approximate formula given by

$$n_s \simeq 1 - 6\epsilon_V + 2\eta_V. \quad (58)$$

The parameter ϵ_V is given by (51) and for η_V we employ (21) from which it follows that

$$\eta_V = \frac{n(n-1 - (n/2+1)ch^n)}{h^2(1+ch^n)}. \quad (59)$$

From this, and ϵ_V of Eq. (51), we get, on account of (58),

$$n_s = 1 - \frac{n^2 + 2n}{h^2}. \quad (60)$$

Replacing h by $h_* = \sqrt{2nN_*}$ a rather simple expression for n_s is obtained given by

$$n_s = 1 - \frac{n+2}{2N_*}. \quad (61)$$

Note that for $n = 2$ and $N_* = 55$ the above formula yields $n_s = 0.9636$ which is well within observational limits but for $n = 4$ a rather large value of N_* is needed to have an acceptable value for n_s . In fact $N_* > 76$ is required to have $n_s = 0.9607$, the lowest allowed if the data $n_s = 0.9649 \pm 0.0042$ is used. This is a rather large value for the number of e-folds N_* . The situation becomes even worse for models with $n > 4$.

It is important, in the framework of this qualitative discussion, to have estimates of the variations of the quantities of interest with varying the parameters of the models at hand. Starting from the power spectrum amplitude, given by (54), it is a trivial task to see that such a variation yields

$$\delta A_s = \left(\frac{\delta\lambda}{\lambda} + \frac{n+2}{2} \frac{\delta N_*}{N_*} \right) A_s. \quad (62)$$

The first term stems from the explicit dependence of A_s on λ . For fixed λ , and varying only a , it is only the second term that contributes. In this case it can be seen that, if the variation of e-folds is of order unity or so, it may produce a substantial change in A_s , of the same order of the errors accompanying the measurements of A_s . Due to the prefactor $(n+2)/2$, on the right hand side of (62), this is larger for models with larger n .

On the other hand, the corresponding variation of the spectral index n_s is found, from (61),

$$\delta n_s = \frac{n+2}{2N_*^2} \delta N_*. \quad (63)$$

This is proportional to the relative change $\delta N_*/N_*$ but is accompanied by an extra N_* in the denominator. Due to that one expects that n_s little varies with changing the number of e-folds.

In order to estimate the variations δN_* , and hence $\delta A_s, \delta n_s$, with varying the couplings involved, namely a and λ for the models under investigation, one should start from Eq (32), and for a fixed value

of the reheating temperature, vary N_* with respect a , λ . The only dependence on these is through the logarithm of $3H_*^2$, which in the slow-roll regime equals to $V_{eff}(h_*)$, and the logarithm involving ρ_{end} . We skip the details of such an analysis. We merely state that the final result is of the form

$$\delta N_* = \frac{\delta a}{a} f_a + \frac{\delta \lambda}{\lambda} f_\lambda, \quad (64)$$

where the factors $f_{a,\lambda}$ depend on the model under consideration.

A last comment regards the instantaneous reheating temperature T_{ins} . This is determined once we know ρ_{end} , see Eq. (31) and discussion following it. With $g_s^{*(reh)} = 106.75$, which we have been using, we have

$$T_{ins} = 0.411 \rho_{end}^{1/4}, \quad (65)$$

which holds in general. However ρ_{end} depends on the details of the model under consideration.

The end of inflation is determined by $\epsilon_1 = 1$, equivalent to $\rho + 3p = 0$. When L - terms are absent this leads to $\rho_{end} = \sigma V_{eff}$, where $\sigma = 1.5$. However, in their presence a more refined analysis is required. Still in this case, the equation $\epsilon_1 = 1$ can be trivially solved, using (15), to give $L\dot{h}^2/K$ in terms of the potential V_{eff} , both evaluated at the end of inflation. That done, it is a fairly easy task to calculate ρ_{end} ,

$$\rho_{end} = \sigma f(c_s) V_{eff}(\bar{h}_{end}) \quad . \quad (66)$$

In this equation, and in order to avoid confusion, we have denoted by \bar{h}_{end} the value of the field at the end of inflation. This depends implicitly on L and can be extracted only numerically. The function $f(c_s)$ depends on the speed of sound squared, c_s^2 , evaluated at the end of inflation, and is given by $f(c_s) = 8c_s^2/(9c_s^2 - 1)$. Due to the fact that $1/3 \leq c_s^2 \leq 1$, as one can see from (34), it is bounded by $1 \leq f(c_s) \leq 4/3$. Had we used the value h_{end} , as this is calculated from $\epsilon_V = 1$, Eq. (66) would have been expressed as,

$$\rho_{end} = \sigma f_\rho V_{eff}(h_{end}) \quad , \quad f_\rho \equiv f(c_s) \frac{V_{eff}(\bar{h}_{end})}{V_{eff}(h_{end})} \quad . \quad (67)$$

This states that the approximate result for ρ_{end} , as given by $\sigma V_{eff}(h_{end})$, is actually dressed by the factor f_ρ . In this factor the function $f(c_s)$ plays no important role, due to the bounds quoted before, but the ratio $V_{eff}(\bar{h}_{end})/V_{eff}(h_{end})$ may deviate substantially from unity. This ratio can be calculated only numerically. However in all models considered, and in a wide range of the parameters, we have found that it lies between $\simeq 0.5$ and 0.65 . Taking, also, into account the bounds on $f(c_s)$, the factor f_ρ lies in the range $0.5 - 0.85$. Due to that the result for ρ_{end} derived numerically is reduced from the approximate result, $\rho_{end} = \sigma V_{eff}(h_{end})$, by the factor f_ρ . For the instantaneous temperature, things are much better since this depends on the quartic root of ρ_{end} . Therefore the numerically derived T_{ins} is smaller by a factor in the range $0.84 - 0.95$. Thus the approximate result $\rho_{end} = \sigma V_{eff}(h_{end})$, which we can derive analytically, yields T_{ins} that are not far from the actual values.

For the models studied in this work, dubbed as Model I, II as well as the Higgs Model, using the equation that relates $L\dot{h}^2/K$ to V_{eff} at the end of inflation, Eq. (66) can be further simplified given by,

$$\rho_{end} = \frac{\sigma}{2a} (1 - c_s^2) \quad , \quad (68)$$

where the speed of sound is meant at the end of inflation. Simple as might be, the value of c_s^2 implicitly depends on the parameters of the model under investigation and it can be calculated only numerically. This is a rather elegant relation, which shows that only c_s at the end of inflation is needed, in order to derive ρ_{end} . It also shows the prominent role of the $L\dot{h}^2/K$, at the end of inflation, through which c_s^2 is determined, see Eq (34). Using (68), the instantaneous reheating temperature can be cast in the form

$$T_{ins} = 0.382 a^{-1/4} (1 - c_s^2)^{1/4} \quad . \quad (69)$$

From this, using the fact that $c_s^2 \geq 1/3$, an absolute upper bound can be derived, $T_{ins} \leq 0.345 a^{-1/4}$, valid for any model considered in this work. From (68), one may be misled to the conclusion that for

large a the instantaneous temperature drops as $a^{-1/4}$. In fact it may drop much faster, due to the implicit dependence of c_s^2 on the parameters involved.

Following the previous discussion, we may derive analytic expressions for the instantaneous temperature, which are good estimates, using the approximate expression $\rho_{end} = \sigma V_{eff}(h_{end})$. For the class of models studied in this subsection, the latter follows from the solution of (52) which depends only on the combination c . Using the analytic form of the potential it is found, in a straightforward manner, that

$$\rho_{end} = \frac{\sigma}{4a} \left(1 - \frac{2}{n^2} h_{end}^2 \right). \quad (70)$$

ρ_{end} , and hence T_{ins} , cannot be quantified further, at this stage, since for this purpose the value of h_{end} is needed. In the following we shall analyze in detail the predictions for this class of models. As already remarked at the beginning of this section, when presenting our final results, for each model considered, we shall solve the pertinent equations numerically using accurate formulas, without approximations, and take into account the temperature dependence of the number of e-folds.

Model I :

We first consider the model (Model I) in which the functions g, M^2 and V are as given by (43) with $n = 2$, that is the potential V is quadratic in the field h ,

$$V(h) = \frac{m^2}{2} h^2. \quad (71)$$

For this case we prefer to use m^2 , instead of λ , since it carries dimension of $mass^2$ when m_P is reinstated. This models has been discussed in [32] and belongs to the class of the cosmological attractors [95], which is clearly seen if one uses the canonically normalized field ϕ , see (19). However no need to do that as we prefer to work directly with the non canonical field h instead. Following the previous findings we define, see Eq. (44), the constant c as the combination

$$c = 2m^2 a. \quad (72)$$

The value of h_* in this case is given by, using (50),

$$h_* \simeq 2\sqrt{N_*}. \quad (73)$$

Then from (55), which arose from the power spectrum amplitude, we get, for values $N_* = 50 - 60$,

$$m \simeq (6.5 \pm 0.5) \times 10^{-6} \quad \text{or} \quad \frac{c}{a} \simeq (8.5 \pm 1.5) \times 10^{-11}. \quad (74)$$

The lowest (largest) limits correspond to $N_* = 60$ ($N_* = 50$). Therefore by using reasonable approximations we derived rather tight limits for the parameter m . Recall that $m^2 \equiv \lambda$ and therefore λ is of the order of 10^{-11} . From the bound (57), which actually arises from the tensor to scalar ratio bound $r < 0.063$, we get, for $N_* = 50 - 60$, a lower bound which is estimated to be in the range,

$$a \geq (0.65 - 0.75) \times 10^8. \quad (75)$$

In this the lowest value corresponds to $N_* = 60$ and the largest to $N_* = 50$. Therefore the parameter a cannot be chosen at will. It should be $\sim 10^8$ or larger. In the following, due to (75), we shall take the largest value as the bound set on a , i.e. $a \gtrsim 0.75 \times 10^8$, which is valid for any N_* in the range of interest.

Concerning the instantaneous reheating temperature, in this case, by solving analytically (52), and replacing h_{end} into (70), we get

$$\rho_{end} = \frac{\sigma}{4a} \left(1 - \frac{\sqrt{1 + 8c} - 1}{4c} \right). \quad (76)$$

We can consider two separate regimes, the small c and the large c , for which ρ_{end} , and consequently T_{ins} , have different dependencies on the parameters involved, as we shall see. Since from (74) the ratio c/a

should be of the order of $\sim 10^{-10}$, small c values are obtained when $a < 10^{10}$. On the other hand large c values are obtained when $a > 10^{10}$.

For small c - values one can expand (76), and using the fact that $\sigma = 1.5$, the instantaneous temperature, as given by (65), receives the form,

$$\rho_{end} \simeq \sigma \frac{c}{2a} = \sigma m^2 \quad \rightarrow \quad T_{ins} = 0.455 \times \sqrt{m}. \quad (77)$$

This, on account of (74), results to a temperature which is $T_{ins} \simeq 2.82 \times 10^{15} GeV$, for $m = 6.5 \times 10^{-6}$. As we shall see this estimate is not far from the one we get in our numerical treatment. What is more important, perhaps, is the fact that in the regime of small c the power spectrum amplitude, which forces m to be within the limits suggested by (74), also determines the maximum reheating temperature.

In the case of large c , ρ_{end} , and hence T_{ins} , have a completely different behavior. In fact in this case, from (76) and (65), we get

$$\rho_{end} \simeq \frac{\sigma}{4a} \quad \rightarrow \quad T_{ins} = 0.321 \times a^{-1/4}, \quad (78)$$

that is, T_{ins} is controlled by the value of a , being proportional to $a^{-1/4}$, and therefore it decreases with increasing a . Due to the fact $a > 10^{10}$, for being within the large c regime, T_{ins} turns out to have values lower than in the small c case. For instance for $a = 10^{12}$ we get from (78) a temperature $T_{ins} \simeq 0.783 \times 10^{15} GeV$ and certainly even lower temperatures for larger values of a . Therefore for having the largest possible value for the instantaneous temperature, of the order $\simeq 10^{15} GeV$, we had better used values $a < 10^{10}$ so that we are within the small c regime.

As already advertised, the cosmological predictions of all models considered are based on a numerical analysis in which no approximation is made. For the model at hand, predictions for three different inputs are presented, named A, B and C, in the following. These correspond to values of the parameters a and c given by $(a, c) = (0.75 \times 10^8, 0.006)$, $(2 \times 10^8, 0.016)$ and $(2 \times 10^9, 0.16)$. These have not been randomly chosen. In fact, for the case A the parameter a touches its lower bound, discussed before, and c has been taken so that m falls well within the range suggested by (74). In fact we choose $m \simeq 6.32 \times 10^{-6}$. The reasoning behind this particular choice for m will be discussed later.

For the other cases larger values of a 's were chosen but the values of c are tuned so that in all cases we have the same value of m , i.e. $m \simeq 6.32 \times 10^{-6}$. In this way we can check how predictions vary with changing the parameter a since we have kept a fixed m . Note that from all cases presented, the case A has the lowest allowed value of a and therefore the Planck upper bound on the tensor to scalar ratio parameter r is almost saturated. The other cases B, C are expected to yield smaller values for r .

In Figure 2, at the top, we display, for the cases A (left) and C (right), the spectral index n_s versus the reheating temperature T_{reh} , for various values of the equation of state parameter ranging from $w = -1/3$ to $w = 1.0$. The shaded region marks the range $n_s = 0.9649 \pm 0.0042$ allowed by observations.

All lines intersect at a common temperature, the instantaneous reheating temperature T_{ins} , marked by thin vertical dashed lines, which for case A equals to $T_{ins} = 2.337 \times 10^{15} GeV$, and for case C to $T_{ins} = 2.099 \times 10^{15} GeV$. Values of reheating temperatures beyond that point, although displayed, are not allowed. The data shown correspond to a pivot scale $k^* = 0.05 Mpc^{-1}$. Note that n_s data by themselves do not impose any restriction on the reheating temperature, as long as the equation of state parameter is in the range from 0.25 to values slightly lower than $\simeq 1.0$. For these values of w any temperature is allowed. For $w < 0.25$ a lower reheating temperature is imposed which is larger for smaller values of w . For instance for the canonical reheating scenario, $w = 0$, this is $\simeq 10^7 - 10^9 GeV$ while for $w = -1/3$ this is $\approx 10^{13} GeV$. At the bottom of the same figure, and for the same set of inputs, the corresponding numbers of e-folds, N_* , are shown, for the A (left) and the C (right) cases respectively.

Note that both n_s and N_* , shown in the figures, are very similar for the two cases, A and C. In particular both observables move slightly downwards in going from A (left) to C (right), that is by increasing the value of a from 0.75×10^8 to 2.0×10^9 , keeping the other parameter fixed. In fact, varying only the parameter a , keeping $\lambda = m^2$ fixed, which is the case for the inputs we are using, we get from (64),

$$\delta N_* = \frac{\delta a}{a} f_a. \quad (79)$$

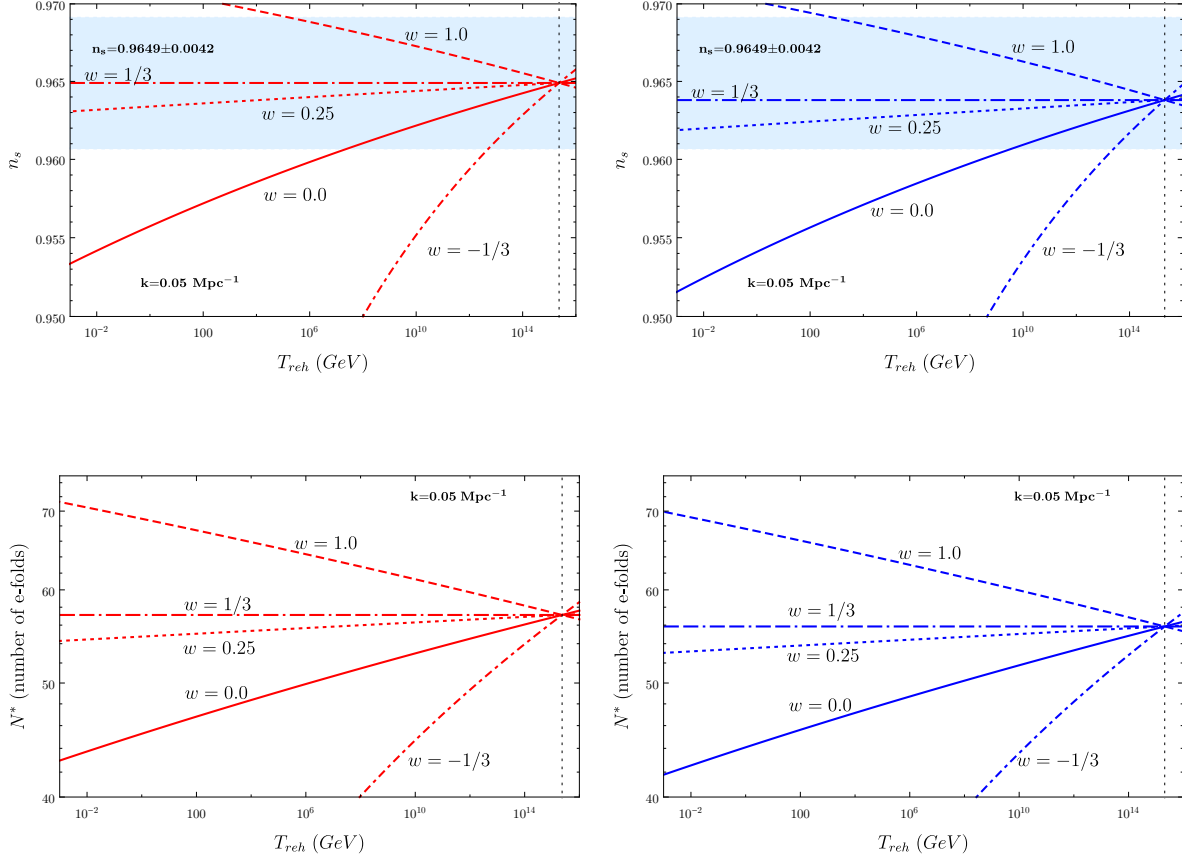


FIG. 2: The spectral index n_s (top) and the number of e-folds N_* (bottom), versus the reheating temperature T_{reh} , in GeV , for a scale $k^* = 0.05 \text{ Mpc}^{-1}$, and for different values of the equation of state parameter, for the cases A (left) and C (right) of Model I, discussed in the text. The shaded region marks the allowed values for the spectral index $n_s = 0.9649 \pm 0.0042$ while the vertical dotted line the instantaneous reheating temperature.

For our input values, we find that the factor f_a is of order unity and negative. The result is that by increasing the value of the parameter a , the relative change $\delta N_*/N_*$, is negative and therefore, due to (63), n_s decreases. This decrease is small, as we have already discussed, what is indeed imprinted on this figure.

The power spectrum amplitude imposes more stringent bounds on T_{reh} than n_s , as shown in Figure 3. In this figure we plot the amplitude $10^9 \times A_s$ versus the reheating temperature T_{reh} , in GeV , for $k^* = 0.05 \text{ Mpc}^{-1}$, and for different values of the equation of state parameter, as in the previous figure. The shaded region marks the allowed range $10^9 \times A_s = 2.10 \pm 0.03$. On the left the case A is shown and on the right the case C. The lines are as in Figure 2. One notices that for the A-case values $w \gtrsim 1/3$ are totally excluded by A_s data while for $w \lesssim 0.25$ limits on the minimum and maximum allowed temperature are imposed. In this case the maximum temperature, for any allowed value of w , can never reach the instantaneous temperature. For the C-case, right panel, one sees, by comparing this figure with the n_s plot, top and right pane of Figure 2, that the bounds set on the reheating temperature are more constrained. In particular, for values of w , which deviate from $w \simeq 1/3$, a lower reheating temperature is established, which is much higher than this imposed by n_s data.

Comparing the two cases, A and C, we observe that A_s also decreases in accord with (62), and the fact

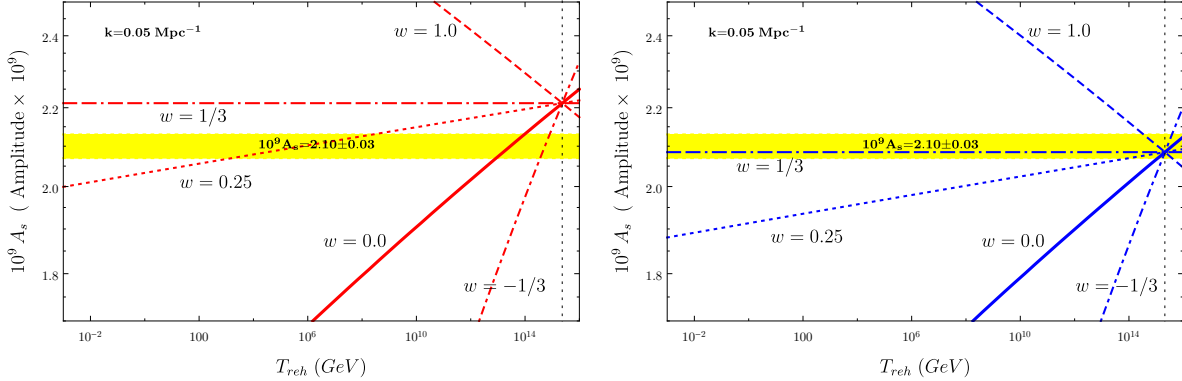


FIG. 3: The amplitude $10^9 A_s$ versus the reheating temperature T_{reh} , in GeV , for $k^* = 0.05 Mpc^{-1}$, for different values of the equation of state parameter. The shaded region marks the allowed values $10^9 A_s = 2.10 \pm 0.03$. On the left the case A is shown and on the right the case C of Model I. The instantaneous temperatures, in each case, are marked by thin dotted vertical lines.

that λ , or equivalently m , is fixed and $\delta N_*/N_*$ is negative. However the change in A_s is relatively large, unlike n_s , in the sense that its variation reaches the order of magnitude of the observational error of A_s , as has been previously discussed.

It is worth mentioning that given a fixed value for the parameter a there is a fine-tuned value of m , in the range suggested by (74), for which the case $w = 1/3$ falls within the allowed region by A_s observations⁶. In this case the instantaneous reheating temperature is determined for any value of w in the range $-1/3 \leq w \leq 1$. However in this case a lowest temperature is determined, which is close to the instantaneous temperature, for any w that deviates from the value $1/3$. This includes the values $0.0 \lesssim w \lesssim 0.25$ which are favored in some reheating scenarios. This can be clearly seen, for instance, in the case C where for $a = 2.0 \times 10^9$ the value $m = 6.32 \times 10^{-6}$ forces the line $w = 1/3$ to be within A_s limits, as shown on the right panel of Figure 3. Keeping a fixed, any slight change in the value of the parameter m , which essentially controls A_s , will move, downwards or upwards, the line $w = 1/3$, off the allowed range, and in this case the instantaneous reheating scenario is no longer supported. At the same time, depending on the value of m , lower and higher limits of reheating temperatures are imposed, different for each w . However some values of w are totally excluded. For instance, by increasing m , the line $w = 1/3$ will be uplifted and move above the upper observational limit set on A_s . In this case all values in the range $1/3 \leq w \leq 1$ are excluded. If, on the other hand m is decreased, the line $w = 1/3$ will move below the lower limit of A_s and values $-1/3 \leq w \leq 1/3$ are excluded. Increasing, or decreasing, further the value of m will exclude all possible cases $-1/3 \leq w \leq 1$. Therefore, there is a range of m outside of which agreement with A_s data can not be obtained, for any value of the equation of state parameter, in the interval $-1/3 \leq w \leq 1$. This range is actually very tight and falls within the suggested range given by (74). Within this range there are fine-tuned values for which reheating can be instantaneous. Note that the sensitivity of the spectral index n_s on the value of m is not that dramatic and n_s data leave more ample space for the observational requirements to be satisfied. Therefore, the conclusion is that given a , the value of m should lie in a very narrow range, in order to comply with power spectrum data. Moreover if reheating is instantaneous it should be fine-tuned accordingly. This, as we shall see, holds for other popular models as well, notably the Higgs model that will be discussed later.

⁶ This requires that the case $w = 1/3$ is compatible with N_* in the range $\approx 50 - 60$, which is always the case provided the parameter a does not take extremely high values.

Model I (pivot scale $k^* = 0.05 \text{ Mpc}^{-1}$)

		A - case			C - case		
w - value		$w = 0.0$	$w = 0.25$	$w = 1.0$	$w = 0.0$	$w = 0.25$	$w = 1.0$
$10^9 A_s$		2.07	2.07		2.07	2.07	2.13
n_s		0.9637	0.9637		0.9637	0.9637	0.9642
r		0.0616	0.0616		0.0040	0.0040	0.0038
N_*		55.25	55.25		55.65	55.65	56.43
T_{reh}		8.542×10^{12}	1.547×10^3		1.138×10^{15}	9.741×10^{13}	3.667×10^{14}
$10^9 A_s$		2.13	2.13		2.08	2.08	2.08
n_s		0.9642	0.9642		0.9638	0.9638	0.9638
r		0.0602	0.0602		0.0039	0.0039	0.0039
N_*		56.03	56.03		55.85	55.85	55.85
T_{reh}		8.861×10^{13}	1.855×10^8		2.099×10^{15}	2.099×10^{15}	2.099×10^{15}

TABLE I: Sample outputs for the Model I, for inputs corresponding to cases A, C (see main text) , for the cosmological observables n_s, r, A_s and N_* , for various values of the equation of state parameter w . The values shown for the reheating temperature T_{reh} , in GeV, correspond to the minimum (upper rows) and maximum (lower rows) allowed, when the observational limits for $A_s \simeq (2.10 \pm 0.03) \times 10^{-9}$ and $n_s = 0.9649 \pm 0.0042$ are imposed. Blank entries indicate that there are no values compatible with the observational bounds put on n_s and A_s , for the specific value of w .

Following the already outlined numerical procedure, in Table I we display sample outputs of the model under consideration for the choice of the parameters corresponding to the inputs A, and C for a pivot scale $k^* = 0.05 \text{ Mpc}^{-1}$. The predicted cosmological observables n_s, r, A_s are displayed, for various values of the equation of state parameter w , corresponding to the minimum (upper rows) and maximum (lower rows) allowed reheating temperatures T_{reh} , when the limits $A_s \simeq (2.10 \pm 0.03) \times 10^{-9}$, and $n_s = 0.9649 \pm 0.0042$ are observed. The corresponding predictions for the number of e-folds N_* , are also shown. Blank entries indicate that there are no values compatible with observational bounds put on n_s, A_s , for the specific value of w . Note that for the C - case, the maximum reheating temperature reaches the instantaneous reheating temperature, $T_{ins} = 2.099 \times 10^{15} \text{ GeV}$. At this temperature predictions are independent of w , due to the fact that T_{ins} marks the intersection of all w -lines. For the same case, the lower limits on T_{reh} are also shown. For the cases $w = 0.0, 0.25$ and $w = 1.0$, these are not very far from the T_{ins} , as already discussed, in agreement with Figure 3, right panel. For the case A, on the other hand, the minimum and maximum reheating temperatures are both smaller than the corresponding ones of the C - case. Note in particular the predictions for $w = 0.25$ for which the range of temperatures, allowed by all observations, is $T_{reh} \simeq (1.5 \times 10^3 - 1.9 \times 10^8) \text{ GeV}$.

In Figure 4 the tensor-to-scalar ratio $r_{0.002}$ versus the spectral index n_s is plotted, for the Model I, for the data set A (red-line), B (green-line) and C (blue-line). In drawing this figure a pivot scale $k^* = 0.002 \text{ Mpc}^{-1}$, was used so that it can be directly compared to the corresponding Planck 2018 bounds [50, 51], which are also drawn. The tiny circle (in magenta), the small (in orange) and the large (in green) correspond to reheating temperatures close to BBN, Electroweak and Leptogenesis scenarios, given by $T_b = 1 \text{ MeV}$, $T_{ew} = 10^2 \text{ GeV}$ and $T_{lep} = 10^9 \text{ GeV}$, respectively. The largest circle (in yellow) marks the instantaneous reheating temperature, see Eq. (31), for each case displayed. The number close to each circle indicates the corresponding number of e-folds left, at the pivot scale $k^* = 0.002 \text{ Mpc}^{-1}$. The value of the equation of state parameter for the figure on top is $w = 0.0$, while for the one at the bottom $w = 0.25$. In the latter only the e-folds corresponding to T_b and the instantaneous reheating are shown, to be clearly visible. In both cases shown, $w = 0$ and $w = 0.25$, the smallest values for the tensor-to-scalar ratio r are obtained in the C-case, that is for the largest values of the parameters a, c . Recall that the ratio c/a has been kept fixed. For smaller values of the parameters, r gets larger and saturates the Planck upper bound in the A - case, corresponding to the lowest allowed values of a, c , as we have already remarked.

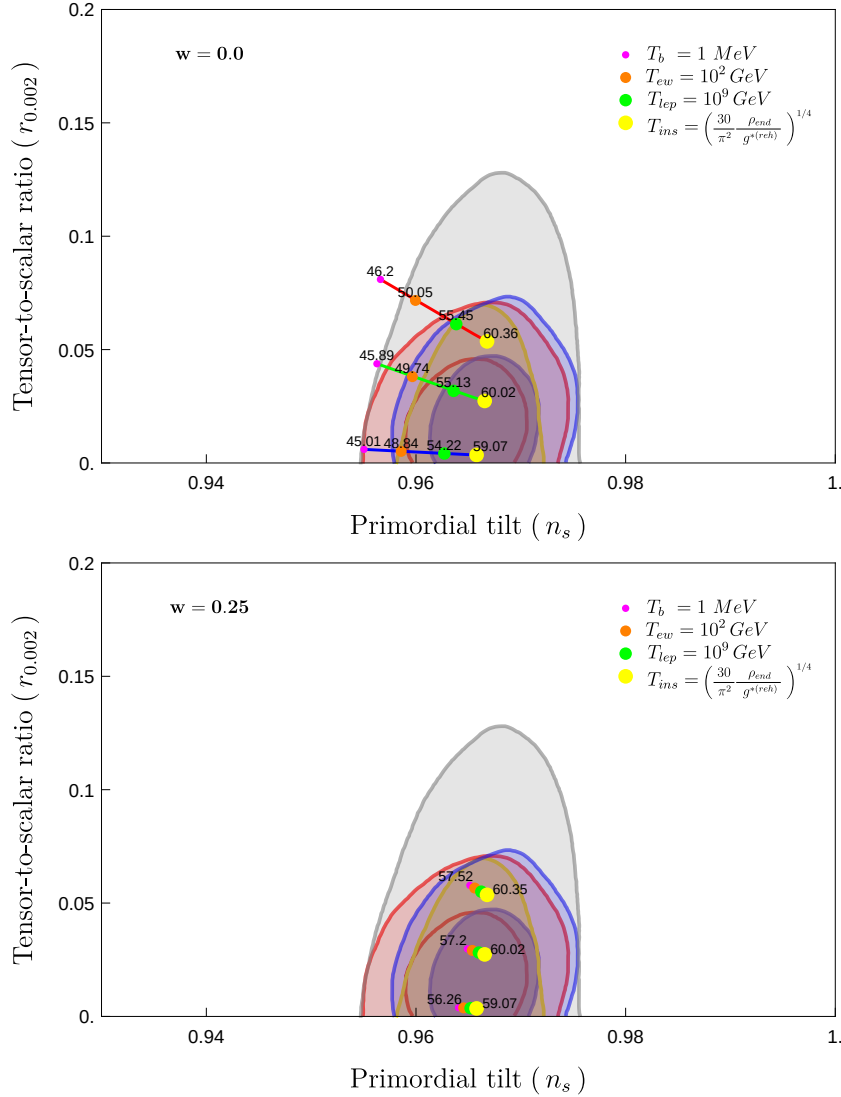


FIG. 4: The tensor-to-scalar ratio $r_{0.002}$ versus the spectral index n_s for the Model I, for the data set A (red-line), B (green-line) and C (blue-line) corresponding to different inputs of the parameters (see main text). A pivot scale $k^* = 0.002 \text{ Mpc}^{-1}$ is used so that a direct comparison with the corresponding Planck 2018 data is possible. The value of the equation of state parameter for the figure on top is $w = 0.0$, while for the figure at the bottom is $w = 0.25$. The tiny circle (in magenta), the small (in orange) and the large (in green) correspond to reheating temperatures close to BBN, Electroweak and Leptogenesis scenarios, while the largest (in yellow) marks the instantaneous reheating temperature (see main text). The numbers indicate the e-folds, in each case, when $k^* = 0.002 \text{ Mpc}^{-1}$.

We point out that in drawing Figure 4 the A_s constraints have not been taken into account. Including these will shrink considerably the allowed line segments, displayed on the figure, since T_{reh} is further constrained by A_s data. For instance, for the C - case, which is well within the region allowed by all observations, yielding also the smallest value for r , a large portion of the segment, with ends corresponding to temperatures T_b and the minimum allowed temperature, as this is read from Table I for each w -case,

will be excised. Only a tiny part of it, close to the maximum reheating temperature T_{ins} , will be left.

Model II :

As a second model (Model II) worth studying, is the one in which the functions g, M^2 are as in (43), as in the Model I, but the potential is quartic in the scalar field involved, i.e.

$$V(h) = \frac{\lambda}{4} h^4, \quad (80)$$

that is $n = 4$. We have already remarked, based on the qualitative arguments presented earlier, that this model, as well as all with $n > 4$, fails to satisfy the observations on the spectral index unless one has a large number of e-folds, probably larger than $N_* > 76$, or so. However a more detailed study is required to get a firm conclusion which also takes into account the reheating temperature.

Using the general results, given at the beginning of this section, when applied to this model, we get ,

$$h_* \simeq \sqrt{8 N_*}. \quad (81)$$

Also on account of (55) the coupling λ is

$$\lambda \simeq 10^{-8} \frac{3.11}{N_*^3}, \quad (82)$$

which for e-folds in the range $N_* = 50 - 60$, yields

$$\lambda \simeq (1.45 - 2.50) \times 10^{-13}, \quad (83)$$

the lowest value corresponding to $N_* = 60$. Therefore the coupling λ must be quite small in order to satisfy the constraints put by observations. As for the parameter a , which sets the inflation scale, employing (57), we have a lower bound given by

$$a \gtrsim (0.95 - 1.00) \times 10^8, \quad (84)$$

not much different from the bounds given in (75).

For T_{ins} we have to calculate h_{end} , as in the $n = 2$ case, and use (70) adapted to the case $n = 4$. Although analytic solution for h_{end} is feasible, through Eq. (52), we will not present it. Instead we shall discuss its behavior for small and large c -values. For small c , omitting $\mathcal{O}(c^2)$ terms, we find $h_{end}^2 \simeq 8(1 - 64c)$. Then from (70) the leading contribution is,

$$\rho_{end} \simeq \sigma \frac{16c}{a} = 16 \sigma \lambda \quad \rightarrow \quad T_{ins} = 0.909 \times \lambda^{1/4}. \quad (85)$$

With $\lambda = 2 \times 10^{-13}$, the central value in the range (83), this yields an instantaneous reheating temperature around $T_{ins} \simeq 1.48 \times 10^{15} GeV$. As in the previously studied model, $n = 2$ case, the power spectrum determines the maximum reheating temperature, in the regime of small c . In the case of large c , h_{end}^2 behaves as $c^{-1/3}$, and hence little contributes to Eq. (70). Then keeping only the leading term in ρ_{end} , we get the same result (78), as in the previous model, and T_{ins} is again proportional to $a^{-1/4}$.

For this model we shall also present sample outputs of our numerical treatment, considering a fixed value $\lambda = 2.0 \times 10^{-13}$, in the middle of the range suggested by (83), and values of a in the range $a = 10^8 - 10^{10}$, respecting therefore the bound (84). The value $a = 10^8$ corresponds to the lowest allowed value, and for future reference we name it A - case, while 10^{10} is arbitrarily taken to be two orders of magnitude larger, which we name B - case. Although, in principle, one can consider larger a - values there is no need to do this for reasons that will be shortly explained.

On the left panel of Figure 5 the predictions for the spectral index n_s , for the cases A (left) and B (right), are shown versus the reheating temperature for various values of the equation of state parameter w . Note that there is no much difference between the two cases, although the parameter a differs by two orders of magnitude. The explanation is the same as that discussed for Model I. Notice that on the right the lines have been moved imperceptibly lower. That is, the tendency is to get lower n_s values as

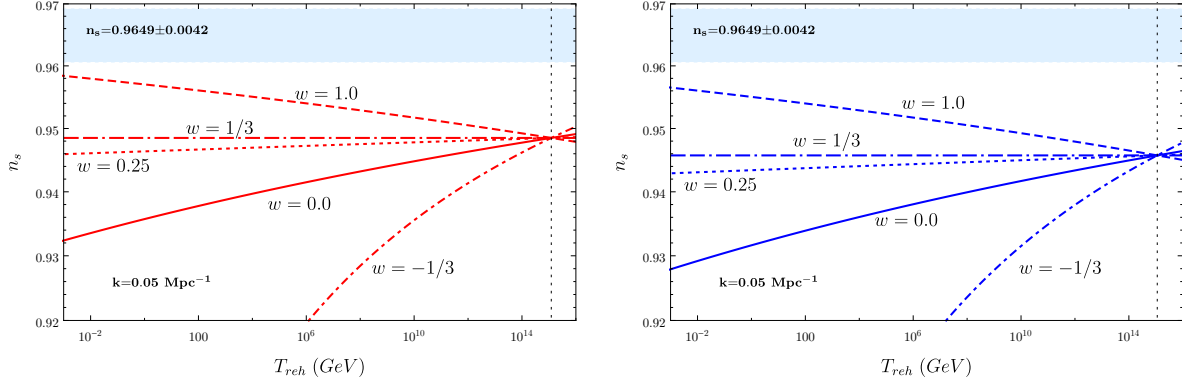


FIG. 5: The spectral index n_s , versus the reheating temperature T_{reh} , in GeV , for a scale $k^* = 0.05 Mpc^{-1}$, and for various values of the equation of state parameter, for the cases A (left) and B (right) of Model II discussed in the text. The shaded regions marks the allowed values for the spectral index $n_s = 0.9649 \pm 0.0042$ and the vertical dotted lines the instantaneous reheating temperatures.

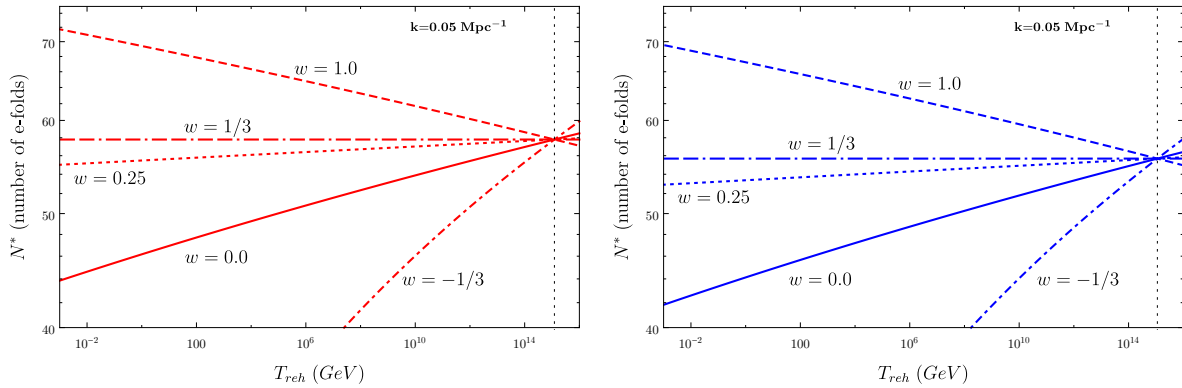


FIG. 6: As in Figure 5 for the number of e-folds N_* .

the parameter a increases. Concerning the instantaneous reheating temperature, for the values taken for a , λ , for the A - case it is $T_{ins} = 1.223 \times 10^{15} GeV$, while for for B - case this is $T_{ins} = 1.129 \times 10^{15} GeV$. These are marked by vertical thin dotted lines, as in previous figures. As already remarked for this model agreement with n_s observational data is hard to achieve. In both cases it is clearly seen from this figure, that only for very small reheating temperatures, and only for $w = 1$, values of n_s that are marginally acceptable can be obtained. In this case the number of e-folds is large $N_* > 70$, as is shown in Figure 6 where the number of e-folds is displayed. This agrees with the general arguments given before, see discussion following Eq. (61). We have not considered larger values of a , since as explained, they would predict lower n_s , resulting to larger deviations from the data.

Although agreement with n_s data cannot be obtained, in this model, for reasons of completeness we shall give a brief account for the predictions for the power spectrum amplitude. Agreement with A_s data requires values of w that are smaller than 0.25, for the A - case, while for the B - case the value $w = 0.25$ is marginally accepted. Values lower than $w \simeq 0.25$ are allowed. Whatever the case, such values for the

equation of state parameter lead, according to Figure 5, to even smaller values of n_s , less than $\simeq 0.945$ or so, and hence unacceptable.

These results are in agreement with [38] where small n_s are also obtained, and indicate that the quartic potential ($n = 4$) is in tension with cosmological data. Models with $n > 4$ yield predictions that according to our general arguments are, also, hard to reconcile with the data.

Therefore the conclusion is that, from the class of the models whose initial potential is of the monomial form $V \sim h^n$, and with constant values for the coefficients of \mathcal{R} and \mathcal{R}^2 terms in the Palatini gravity, only the case $n = 2$, which belongs to the class of the cosmological attractors [95], can lead to successful inflation, if all observational constraints are taken into account.

B. Non-minimally coupled models

A non-minimal coupling arises if in the previously studied models the constants g and/or M^2 are promoted to be field dependent. A particularly interesting case is the model in which

$$g(h) = 1 + \xi h^2, \quad M^2(h) = \frac{1}{3a}, \quad V(h) = \frac{\lambda}{4} h^4. \quad (86)$$

This belongs to the class of models (43), with quartic potential, however the scalar h is non-minimally coupled to the scalar curvature \mathcal{R} , in the Palatini framework, since g is field dependent, in the particular way shown above. This model arises actually from the Higgs coupling to Palatini gravity

$$\frac{m_P^2 + 2\xi H^\dagger H}{2} \mathcal{R} + \frac{a}{4} \mathcal{R}^2 + |DH|^2 - \lambda \left(|H|^2 - \frac{u^2}{2} \right)^2, \quad (87)$$

where $u \simeq 246 \text{ GeV}$ is the Electroweak scale. In Planck units, $m_P = 1$, this is very small $u \sim 10^{-16}$ and plays no significant role in inflation. Setting therefore $u = 0$ and working in the unitary gauge, $H^\dagger = (0, h/\sqrt{2})$, (87) is actually the model described by g, M^2 and quartic potential as given in (86).

The Higgs coupling to gravity and its role as the inflaton, in the metric formulation, has been proposed in [96, 97] and it has been widely studied since then [29, 32, 33, 36, 38, 44, 98–119] both in the context of the metric formulation and in Palatini formulation. The importance of the \mathcal{R}^2 term in (87) has been discussed in [32, 33, 36, 38]. In this work we shall show that the quartic coupling λ , as in the minimally coupled quartic model studied previously, corresponding to $\xi = 0$, is constrained considerably by cosmological data, especially the power spectrum amplitude A_s . This limits the available options especially when the reheating of Universe after inflation is taken into account.

The functions K, L and V_{eff} in this model are given below, in the limit $u = 0$,

$$K(h) = \frac{1 + \xi h^2}{(1 + \xi h^2)^2 + ch^4}, \quad L(h) = \frac{a}{(1 + \xi h^2)^2 + ch^4}, \quad (88)$$

while the potential V_{eff} receives the form

$$V_{eff}(h) = \frac{1}{4a} \frac{ch^4}{(1 + \xi h^2)^2 + ch^4}. \quad (89)$$

As in the simple quartic potential the parameter c is the combination $c = a\lambda$. Notice however that a non-trivial ξ -dependence exists and therefore the Higgs model differs from the simple quartic model studied previously. Evidently when $\xi = 0$ the functions (88), (89) smoothly go into (45), (46)

For large values of h the potential (89) approaches a plateau $\simeq 1/4(a + \xi^2/\lambda)$, and therefore an inflation scale μ can be set. In particular, reinstating units, this is defined by $\mu \equiv m_P/\sqrt{3(\xi^2/\lambda + a)}$. Then for large field values the potential approaches $V_{eff} \simeq 3\mu^2 m_P^2/4$. For comparison, in the Starobinsky model the inflaton potential reaches the value $3\mu_S^2 m_P^2/4$, where μ_S is the scalaron mass, and in that case cosmological data determine its magnitude, given by $\mu_S \simeq 10^{-5} m_P$. In the model under consideration, the magnitude of μ will be discussed later, when imposing limits on the parameters ξ, λ and a .

Proceeding in the same manner, as in the previously studied models, the slow - roll parameters ϵ_V, η_V are given by, as functions of h ,

$$\epsilon_V = \frac{8(1 + \xi h^2)}{h^2(1 + 2\xi h^2 + (\xi^2 + c)h^4)}, \quad \eta_V = \frac{4}{h^2} \left(-\frac{3 + 2\xi h^2}{1 + \xi h^2} + \frac{6(1 + \xi h^2)}{(1 + \xi h^2)^2 + ch^4} \right). \quad (90)$$

Although the parameter η_V has a rather complicated form both the spectral index and the power spectrum amplitude have rather simple expressions. In fact they are given by

$$n_s = 1 - \frac{16}{h_*^2} - \frac{8}{h_*^2(1 + \xi h_*^2)} \quad (91)$$

and

$$A_s = \frac{\lambda}{24\pi^2} \frac{h_*^6}{32(1 + \xi h_*^2)}, \quad (92)$$

where we have replaced the field h by its pivot value h_* . These coincide with (60) and (47), respectively, for $n = 4$, when $\xi = 0$, as they should. However, the presence of the ξ alters the predictions for the cosmological observables, as we shall see.

In order to proceed further we need the pivot value h_* . In this case the number of e-folds N_* is given by

$$N_* = \frac{1}{8} (h_*^2 - h_{end}^2). \quad (93)$$

This does not depend explicitly on the parameter ξ and is identical with (49) when $n = 4$. Therefore

$$h_*^2 = 8N_* + h_{end}^2, \quad (94)$$

which is functionally the same as (50) but the value of h_{end} differs. The latter depends on both ξ and the combination $c = a\lambda$, being determined as solution of the equation

$$c h_{end}^6 + (1 + \xi h_{end}^2)(h_{end}^2(1 + \xi h_{end}^2) - 8) = 0. \quad (95)$$

This is a cubic equation in h_{end}^2 , which we prefer to cast it in the form (95) for reasons that will become clear in the following. Notice that in the limit $\xi = 0$ this equation becomes (52), when in the latter we put $n = 4$. In the form presented by (95) we see that when $c = 0$ the solution for h_{end}^2 is easily obtained since it becomes a quadratic equation for h_{end}^2 . This observation is useful if we want to study the predictions of the model for small c , and in doing that we expand in powers of c about the zeroth order solution.

Being a cubic equation for h_{end}^2 , analytic solution can be obtained, and in our case there is only one real and positive solution. The value of this solution, for h_{end}^2 , can never exceed 8. In fact this value is reached when ξ, c are smaller than $\sim 10^{-3}$, or so. For larger values the root of this equation is smaller. The conclusion is that h_{end}^2 can be neglected in (94) and h_* can be approximated by

$$h_* \simeq \sqrt{8N_*}, \quad (96)$$

as in the simple quartic model. Replacing this value in (91) and (92) we get

$$n_s = 1 - \frac{2}{N_*} - \frac{1}{N_*(1 + 8\xi N_*)}, \quad (97)$$

and

$$A_s = \frac{2\lambda}{3\pi^2} \frac{N_*^3}{(1 + 8\xi N_*)}. \quad (98)$$

As expected in the limit $\xi = 0$ these smoothly go to (61) and (54) when in the latter we put $n = 4$.

However the role of the parameter ξ is very important and can improve the case, as far as the spectral index n_s is concerned. In the simple quartic model the predictions for n_s are hard to comply with the cosmological observations, unless large values of the e-folds are considered, $N_* > 70$ or so, as already discussed. This has been also pointed out in [32, 33]. Such large values of e-folds may not be acceptable, since they demand very low values for the reheating temperature, at least in the standard reheating scenarios. Accepting large number of e-folds, $N_* > 70$, it may be consistent with alternative reheating scenarios, which may be interesting per se, however, in this work we would prefer to keep a more conservative attitude.

Concerning ξ , we shall assume that it is positive. Then one sees from (97) that n_s is larger than the one obtained in the quartic potential studied before, which corresponds to $\xi = 0$. Moreover, for any N_* the observable n_s increases as ξ grows and therefore values within limits may be obtained for sufficiently large values of ξ . From (97) it can be seen that for values $\xi \simeq 0.06$ the spectral index can be within observational limits, for e-folds in the range $N_* \simeq 52 - 60$. That is for this value of ξ a large portion of e-folds, in the range $50 - 60$, is covered, which is broadened for larger ξ allowing, also, for values of N_* lower than 52. Values of $\xi < 0.06$ are also acceptable, at the cost of shrinking considerably the range of the allowed e-folds, that are compatible with the observational limits imposed by n_s . For instance for $\xi \simeq 0.004$ one obtains $n_s = 0.9607$, at the edge of the lower observational limit, pushing N_* to $N_* \simeq 60$. From these arguments it is obvious that a reasonable range to deal with in our numerical procedure is to focus on values of ξ of the order of $\mathcal{O}(10^{-2})$, or larger. In the following we shall take $\xi \gtrsim 0.06$ on the grounds that is likely to cover a wider range of e-folds, as we explained above.

From (98), and accepting that $A_s \simeq 2.1 \times 10^{-9}$, the quartic coupling is found to be constrained by

$$\lambda \simeq 3.11 \times 10^{-8} \frac{1 + 8\xi N_*}{N_*^3}. \quad (99)$$

In the limit $\xi = 0$ this coincides with (82), as it should. From this it is seen that the allowed values for λ depend on the parameter ξ , and also that larger values of the coupling λ , as compared to the simple quartic model, are available in this case. However even in this case the quartic coupling is small. For $\xi = 0.06$ it is of order $\sim 10^{-12}$. In order for λ to reach values of order $\gtrsim 10^{-6}$ one needs large values $\xi \gtrsim 10^4$, when $N_* \simeq 50 - 60$.

Concerning the parameter a , by the same token, as discussed in previous models, a lower limit on it can be established by (41), given by

$$a \gtrsim 10^8 \left(1.25 - \frac{N_*(1 + 8\xi N_*)}{200} \right). \quad (100)$$

This bound on a depends on ξ , it is quadratic in N_* , and there is a critical value of ξ beyond which it becomes negative, signaling that in this case any positive value of a is actually allowed. As we prefer to work with values $\xi > 0.06$ the rhs of (100) is negative, for $N_* \simeq 50 - 60$, and practically for our purposes there is no lower limit imposed on the parameter a . The absence of a lower bound may be important since in this case a can be chosen either larger, or smaller, than the ratio ξ^2/λ . In the regime

$$\xi^2 > a \lambda, \quad (101)$$

an upper bound on a is imposed, for given ξ, λ . Of particular interest, within this regime, is the case where $\xi^2 \gg a \lambda$. In this limit, it is seen from (88) and (89) that the functions $K(h)$ and the potential $V_{eff}(h)$ do not depend on the parameter a . In fact $K(h)$ depends only on ξ and $V_{eff}(h)$ on ξ, λ . The function $L(h)$ does depend on a , however, its effect in the equations of motion is small, for the cases of interest, as we have already remarked in Section III. Therefore in this case the results are independent of the parameter a , as long as $\xi^2 \gg a \lambda$ holds. This we have verified in our numerical procedure. In this case the inflation scale μ , as defined before (see discussion following Eq. (89)), becomes $\mu \simeq \sqrt{\lambda/3\xi^2} m_P$ and lies in the range $\sim (2 \times 10^{-5} - 5 \times 10^{-7}) m_P$, for values of ξ in the range $0.06 - 100.0$ and for N_* between $50 - 60$, the smaller (larger) scales being attained for higher (lower) ξ and N_* values.

Evidently the arguments given before are no longer valid if the parameters are chosen in the regime

$$\xi^2 < a \lambda. \quad (102)$$

ξ	λ	ξ^2/λ	$a > \xi^2/\lambda$	$a < \xi^2/\lambda$
10^ν	$10^{-10+\nu}$	$10^{10+\nu}$	$> 10^{10+\nu}$	$< 10^{10+\nu}$

TABLE II: Order of magnitude estimates for λ , and ξ^2/λ , as derived from Eq. (99), for given value of ξ (first row) and value of e-folds $N_* = 50 - 60$. In the fourth (fifth) column the lower (upper) bound, set on the parameter a , is displayed for having $a > \xi^2/\lambda$ ($a < \xi^2/\lambda$). The power ν is positive, for $\xi > 1$, and negative for $\xi < 1$.

Then we have a lower bound on a , for given ξ, λ . In this case the predictions depend on a and ξ, λ as well. In particular, when $\xi^2 \ll a\lambda$ the inflation scale is $\mu \simeq m_P/\sqrt{3a}$, that is it is determined solely by a .

For facilitating the discussion, in Table II we present order of magnitude estimates of the quartic coupling λ , as these arise from (99), and the corresponding ξ^2/λ for given value of $\xi = 10^\nu$, where $\nu < 0$ or $\nu > 0$, corresponding to $\xi < 1$ or $\xi > 1$, respectively. We see that the coupling λ increases with increasing ξ , or same, increasing ν . Although not displayed in the table, we remark that for $\nu \geq 0$ the coupling λ lies within $(0.7 - 1.0) \times 10^{-10+\nu}$. The lower and upper bounds on the parameter a , for having $a > \xi^2/\lambda$ and $a < \xi^2/\lambda$, are shown in the fourth and fifth column, respectively. In creating this table the values of N_* were taken, as usual, in the range $N_* \simeq 50 - 60$.

In order to have an estimate of the instantaneous reheating temperature, T_{ins} , which is given by (65), we need know the energy density at the end of inflation. Following similar arguments, as for the models studied previously, we find that in this case it is given by

$$\rho_{end} = \frac{\sigma}{4a} \left(1 - \frac{h_{end}^2(1 + \xi h_{end}^2)}{8} \right) \equiv \frac{\sigma}{4a} F(\xi, c). \quad (103)$$

Recall that $\sigma = 1.5$. The function $F(\xi, c)$ is too complicated to be presented, although analytic expression for the unique positive solution h_{end}^2 of Eq. (95) does exist. This we shall actually use for the calculation of ρ_{end} through (103). Replacing a by c/λ , with λ as given by (99), we get from (65),

$$T_{ins} = (0.968 \times 10^{-3}) \left(\frac{55}{N_*} \right)^{1/2} \left(\xi + 2.27 \times 10^{-3} \frac{55}{N_*} \right)^{1/4} R^{1/4}(\xi, c), \quad (104)$$

where $R(\xi, c) = F(\xi, c)/c$. This it gets a very simple form in particular regions, and interestingly enough this includes the region where T_{ins} gets its largest value.

The first region of interest is when $c/\xi^2 < 1$. As we have already remarked, Eq. (95) is easily solved when c vanishes, since in that case it is reduced to a quadratic equation for h_{end}^2 . For non-vanishing c , within the regime $c/\xi^2 < 1$, we can treat this ratio as a small parameter, in order to find the desired solution as deviation from the zeroth-order solution, corresponding to $c = 0$. This is easily implemented, resulting to a function $R(\xi, c)$, which to the lowest order in c/ξ^2 , is independent of c . In particular it is found that,

$$R(\xi, c) = \left(\frac{1 + 16\xi - \sqrt{1 + 32\xi}}{16\xi^2} \right)^2 \equiv P(\xi). \quad (105)$$

The function $P(\xi)$ is regular at $\xi = 0$, with limit $P(0) = 64$. Using this, we find from (104)

$$T_{ins} = (0.968 \times 10^{-3}) (\xi P(\xi))^{1/4}. \quad (106)$$

In this we have set $55/N_* \simeq 1$, and, besides, we assume that $\xi > 0.01$, which is actually the region we are interested in. Note that (106) is valid in the regime $c/\xi^2 < 1$ and it is a very handy relation. Within the $c < \xi^2$ regime the maximum temperature is attained when $\xi P(\xi)$ reaches its maximum. This occurs at $\xi = 3/32$, that is very close to $\simeq 0.094$, and for this value $T_{ins} \simeq 2.47 \times 10^{15} GeV$, in natural units. This is independent of c as long as c is much smaller than ξ^2 . Away from this maximum T_{ins} drops, as ξ increases, behaving as $T_{ins} \simeq (0.968 \times 10^{-3}) \xi^{-1/4}$.

Another region of interest is when c is large and $c \gg \xi^2$. In this region the function $F(\xi, c)$, that controls ρ_{end} in (103), is very close to unity. Note that the largeness of c by itself is not adequate to

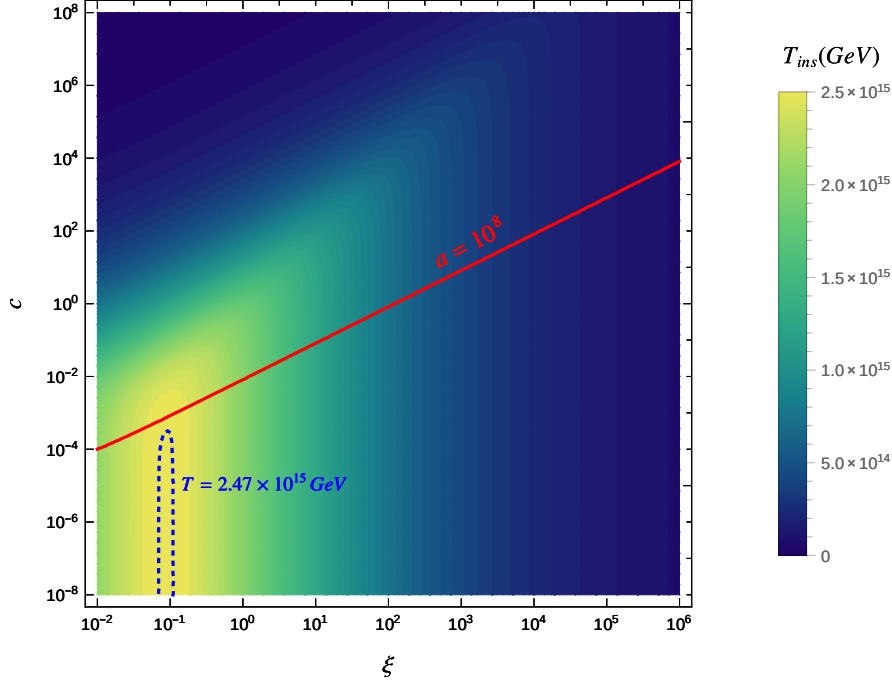


FIG. 7: In the c, ξ plane we display the instantaneous reheating temperature, as given by Eq. (104), for $N_* = 55$. Light colors correspond to larger temperatures. The largest temperature, $T \simeq 2.47 \times 10^{15} \text{ GeV}$, is within the yellow region near $\xi \simeq 0.1$, with boundary the blue dashed line. The red line is the locus of points with $a = 10^8$.

have $F(\xi, c) \simeq 1$, despite the fact that h_{end}^2 is small. We must require, in addition, that $c \gg \xi^2$. Then ρ_{end} turns out to be inverse proportional to a , and hence the instantaneous reheating temperature is proportional to $a^{-1/4}$, or same proportional to $(\lambda/c)^{1/4}$. The latter is proportional to $(\xi/c)^{1/4}$, when (99) is used. Then the analytic result for T_{ins} , in this case, is trivially found from (104),

$$T_{ins} \simeq (0.968 \times 10^{-3}) \left(\frac{\xi}{c} \right)^{1/4}. \quad (107)$$

This holds for large c values, satisfying $c \gg \xi^2$, and therefore it cannot be arbitrarily large. The largest value within this regime is about $\simeq 10^{15} \text{ GeV}$, which is slightly smaller than the corresponding temperature of the $c \ll \xi^2$ region. This is obtained for $c \simeq 10^2$, which is relatively large, and values of ξ^2 about an order of magnitude smaller than c . Any other pair of values, for these parameters, within this particular regime, results to lower values of T_{ins} .

Unfortunately, outside the aforementioned regions there are not simple mathematical expressions to deal with, and we shall rely on a numerical treatment of (104). In fact scanning the two dimensional parameter space c, ξ^2 we found, that the approximate formulas given before in the appropriate regions, agree to a very good accuracy with the values obtained from (104). In Figure 7 we display the instantaneous reheating temperature, as given by Eq. (104), for $N_* = 55$. Light colors correspond to higher temperatures. From this figure it is clearly seen that the larger temperatures are obtained for values of the parameters within the small yellow region, located at the bottom and left. The region with the largest temperature T_{ins} is centered about $\xi \simeq 0.1$, and values $c \lesssim 10^{-4}$, having as boundary the blue dashed line corresponding to $T_{ins} = 2.47 \times 10^{15} \text{ GeV}$. The maximum temperature attained is very close to it, confirming, therefore, our previous arguments. Within this region $\xi \simeq 0.1$, and since Eq. (99) is used, $\lambda \simeq 10^{-12}$. Therefore $a = c/\lambda \lesssim 10^8$ is needed for having the largest possible T_{ins} . This is also seen by drawing the locus of points for which the parameter a has a constant value, $a = 10^8$. This lies

just above the aforementioned region. Lower values, $a < 10^8$, will move this line downwards, crossing the largest T_{ins} region, and thus the maximum T_{ins} is obtainable.

Note that the analytic expressions for T_{ins} , given so far, serve as an estimate of the magnitude of the instantaneous temperature. As we have already pointed out, the actual values are extracted by solving the pertinent equations of motion numerically. However, the numerical analysis reveals that these estimates are accurate enough. In fact, the results derived are lower by less than about 10%. Only in a small region, for $c \leq 10^{-8}$ and for ξ values in the vicinity $\xi \simeq 0.1$, this difference augments to about 15%, or so. This is in accord with the discussion following Eq. (67). As a result the maximum instantaneous reheating temperature mentioned before, $T_{ins} = 2.47 \times 10^{15} \text{ GeV}$, drops to $T_{ins} = 2.07 \times 10^{15} \text{ GeV}$.

Our numerical study can be summarized by selecting the following representative inputs :

For the value $\xi = 0.06$, which according to preceding discussion sets the threshold for having sufficient number of e-folds, we choose the quartic coupling $\lambda = 4.875 \times 10^{-12}$. From (99) one can see that for $N_* = 50 - 60$ the quartic coupling is between 4.29×10^{-12} (for $N_* = 60$) and 6.22×10^{-12} (for $N_* = 50$), so that the value chosen is indeed within the appropriate range. However, this fine-tuned value has been chosen so that the predicted amplitude A_s is within observational limits, in such a way that instantaneous reheating is feasible. It should be remarked that the approximate formula used for A_s may differ from the one that the numerical procedure returns. The latter yields more accurate results, since the exact numerical solution for the field h is used, and also, because it incorporates corrections, see Eq. (25), that although small in some cases are of the same order of magnitude with the observational errors. It is for this reason that fine-tune adjustments are necessary to make the instantaneous reheating mechanism a viable possibility.

For these inputs $\xi^2/\lambda \simeq 7.38 \times 10^8$, and therefore for values $a \ll 10^8$ we are in the regime $a \ll \xi^2/\lambda$ and, as we have discussed, predictions are insensitive to the choice of a . Therefore any value of a yields the same results, provided $a \ll 10^8$. This we have verified by our numerical code. For definiteness we take $a = 10^6$ which is three orders of magnitude smaller than ξ^2/λ given above.

In Figure 8, at the top, we display the spectral index and the power spectrum amplitude. We see that agreement with n_s data is obtained for any temperature when the parameter w is $\simeq 0.25$ or larger, but smaller than 1.0. For canonical reheating, $w = 0.0$, however a lower bound is imposed $T_{reh} \gtrsim 10^{10} \text{ GeV}$, while for $w = 1.0$ the lower bound is about $T_{reh} \gtrsim 100 \text{ GeV}$. Looking at A_s plot we observe, as advertised, that instantaneous reheating can occur, for the given ξ, λ inputs. We also observe that the constraints are more stringent than those imposed by n_s . In fact values of $w > 1/3$, allow for temperatures which are very close to T_{ins} . At the same time a lower reheating temperature is imposed for the $w = 0.25$ case, $T_{reh} \gtrsim 10^{11} \text{ GeV}$, while for the canonical scenario the lower limit imposed by A_s is pushed to a much higher value, close to T_{ins} . At the bottom of the same figure the number of e-folds is shown. Although values of e-folds N_* as large as $\simeq 70$ for low T_{reh} are allowed, by n_s data, when $1 > w \geq 0.25$, the A_s measurements restrict the allowed temperature range in such a way that N_* is forced to be in the range $\simeq 55.70 - 56.30$, as shown in Table III. In this table the predictions for A_s, n_s, r, N_* , corresponding to the minimum (upper rows) and maximum (bottom rows) reheating temperature, are also shown. The maximum reheating temperature is the instantaneous temperature, $T_{ins} = 2.027 \times 10^{15} \text{ GeV}$, and for this reason the predictions for the various w , in that case, coincide.

As a second sample we consider values of ξ in the range $\xi = 0.06 - 10.0$ when the parameter a is increased to $a = 10^{12}$. These cases fall in the regime $a > \xi^2/\lambda$ when λ is within the range suggested by (99). Following the same reasoning, we may consider values for the quartic coupling so that agreement with A_s data is obtained, requiring, at the same time, the maximum reheating temperature can reach the instantaneous temperature T_{ins} . For the lowest value of ξ in this range, $\xi = 0.06$, the quartic coupling can be taken $\lambda = 5.60 \times 10^{-12}$ while for the largest, $\xi = 10$, the value $\lambda = 8.85 \times 10^{-10}$ suits our needs. For reference, these cases we shall name A and B, respectively.

Note that by changing a , from $a = 10^6$ to $a = 10^{12}$, the predicted values for the cosmological parameters change as well, and thus readjustments of λ are necessary, in order to obtain agreement with A_s data, and have, at the same time, T_{ins} as the maximum temperature. This is the reason the values of λ , for the case $\xi = 0.06$, are slightly different for $a = 10^6$ and $a = 10^{12}$.

In Figures 9 and 10 we display the predictions for the spectral index and the power spectrum amplitude for the cases A and B, respectively, discussed before. Comparing Figure 9 with Figure 8 (on top) we first observe that T_{ins} is lowered, in comparison to the A - case. In fact, from $T_{ins} = 2.027 \times 10^{15} \text{ GeV}$

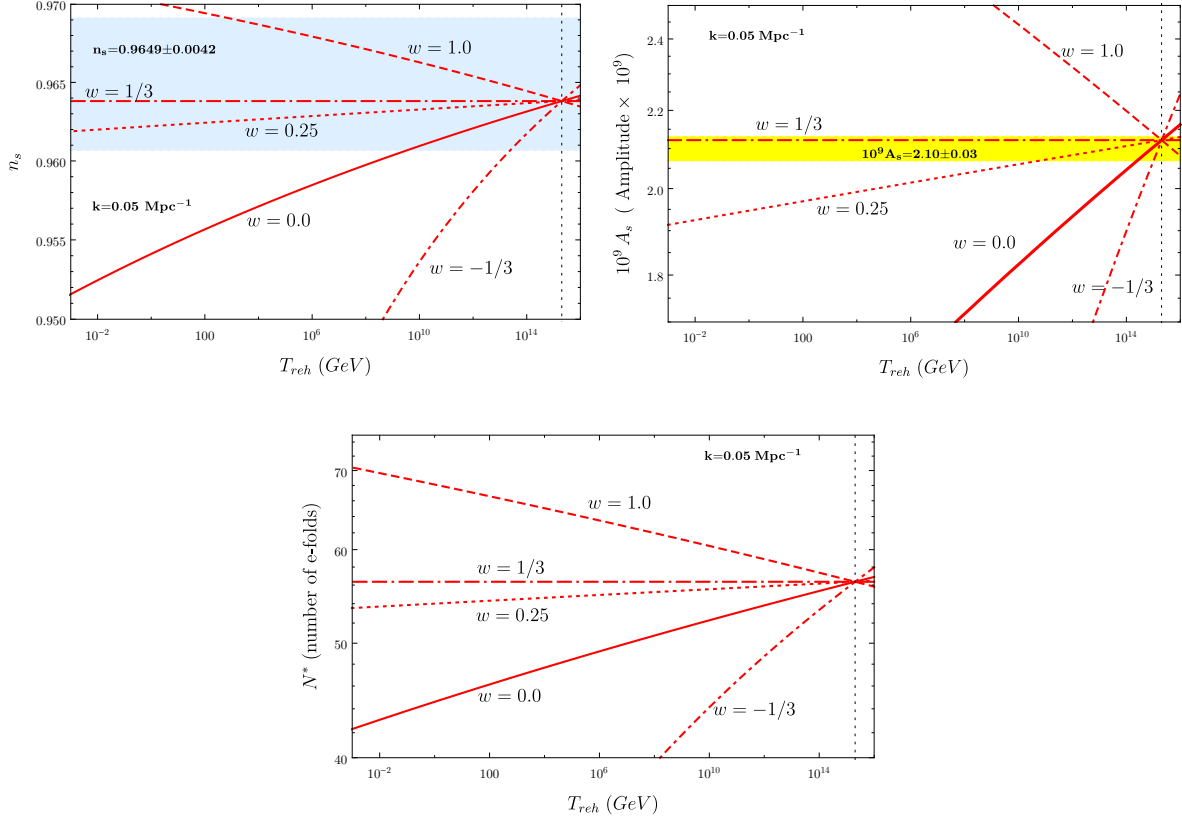


FIG. 8: Top: The spectral index n_s , left, and the power spectrum amplitude A_s , right, versus the reheating temperature T_{reh} , for the Higgs model, for inputs $\xi = 0.06$, $\lambda = 4.875 \times 10^{-12}$ and $a = 10^6$. Bottom: For the Higgs models and same inputs, the number of e-folds versus the reheating temperature T_{reh} is displayed.

Higgs Model (pivot scale $k^* = 0.05 \text{ Mpc}^{-1}$)

Input values	$\xi = 0.06$	$\lambda = 4.875 \times 10^{-12}$	$a = 10^6$
w - value	$w = 0.0$	$w = 0.25$	$w = 1.0$
$10^9 A_s$	2.07	2.07	2.13
n_s	0.9634	0.9633	0.9639
r	0.0102	0.0102	0.0100
N_*	55.67	55.67	56.45
T_{reh}	2.562×10^{14}	6.695×10^{10}	1.569×10^{15}
$10^9 A_s$	2.12	2.12	2.12
n_s	0.9638	0.9638	0.9638
r	0.0100	0.0100	0.0100
N_*	56.36	56.36	56.36
T_{reh}	2.027×10^{15}	2.027×10^{15}	2.027×10^{15}

TABLE III: Predictions of the Higgs Model, for the input values shown on the top, for the cosmological observables n_s, r, A_s, N_* and for various values of the equation of state parameter w . The values shown for the reheating temperature T_{reh} , in GeV, correspond to the minimum (upper rows) and maximum (lower rows) allowed, when the observational limits for A_s and n_s are imposed.

it slides down to $6.522 \times 10^{14} \text{ GeV}$. Also the lowest reheating temperatures change a little. For instance for $w = 0.25$ this is 1.065×10^{11} , i.e. it has been slightly increased from the corresponding $a = 10^6$ case, which was 6.695×10^{10} (see Table III). In Figure 10 the corresponding predictions for the B - case are shown. In this case $T_{ins} = 6.647 \times 10^{14} \text{ GeV}$. That is, it is slightly larger than the case A. Keeping a fixed the tendency for T_{ins} is to decrease, with increasing the parameter ξ , as long as $a > \xi^2/\lambda$, while tuning the quartic coupling to have agreement with A_s data.

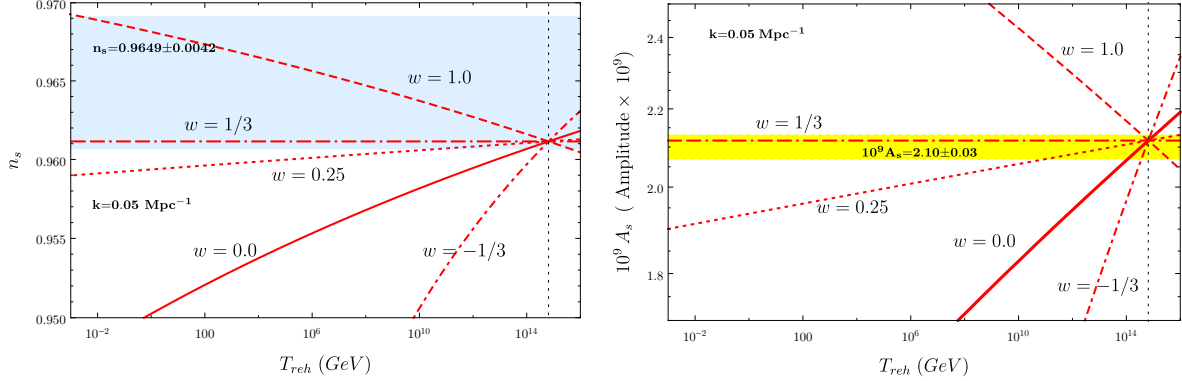


FIG. 9: The spectral index n_s , left, and the power spectrum amplitude A_s , right, versus the reheating temperature T_{reh} , for the Higgs model, for inputs $\xi = 0.06$, $\lambda = 5.6 \times 10^{-12}$ and $a = 10^{12}$ (case A).

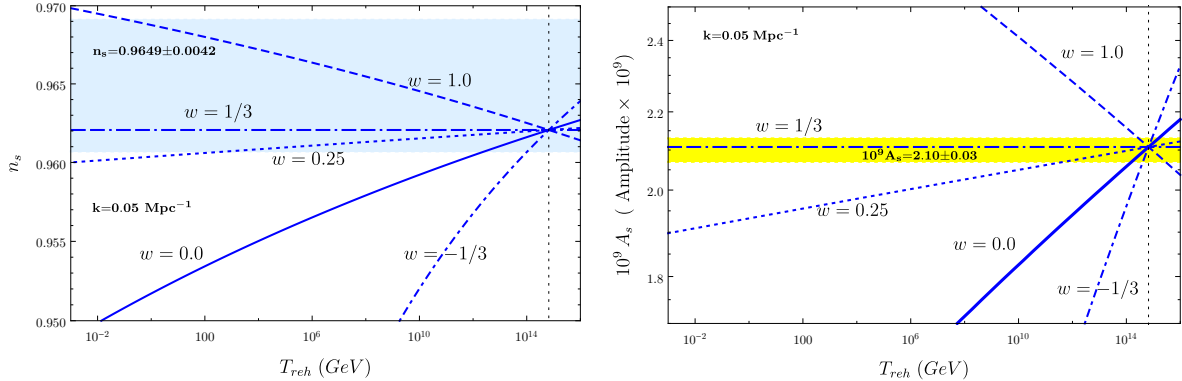


FIG. 10: The same as in Figure 9, for inputs $\xi = 10.0$, $\lambda = 8.85 \times 10^{-10}$ and $a = 10^{12}$ (case B).

In Figure 11, we show the tensor-to-scalar ratio $r_{0.002}$ versus the spectral index n_s for the Higgs model. The numbers of the e-folds are shown, and the circles designate different reheating temperatures, exactly as in Figure 4. The upper line (in red) corresponds to parameters $a = 10^6$, $\xi = 0.06$ and $\lambda = 4.875 \times 10^{-12}$ while for the one at the bottom (in blue) the parameters are $a = 10^{12}$, $\xi = 0.06$ and $\lambda = 5.60 \times 10^{-12}$. Only the cases for the canonical reheating are shown, i.e. $w = 0$. Note that in drawing this figure the constraints arising from A_s have not been taken into account. When they are a small segment including the T_{ins} temperature is left. In any case, we observe from these figures that by increasing the parameter a the tensor-to-scalar ratio gets smaller and the predictions move lower and

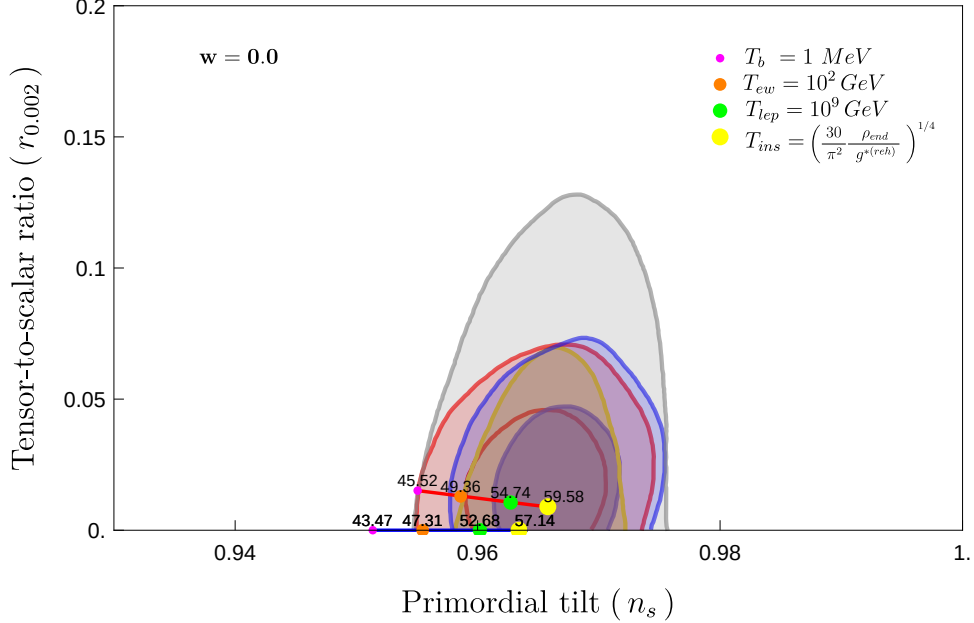


FIG. 11: The tensor-to-scalar ratio $r_{0.002}$ versus the spectral index n_s for the Higgs. As in Figure 4 the numbers shown correspond to the e-folds and the circles designate different reheating temperatures. For the line on top (in red) the parameters are $a = 10^6$, $\xi = 0.06$ and $\lambda = 4.875 \times 10^{-12}$ while for the one at the bottom (in blue) $a = 10^{12}$, $\xi = 0.06$ and $\lambda = 5.60 \times 10^{-12}$. Only the cases for the canonical scenario are shown, $w = 0$.

the instantaneous reheating temperature mechanism is in full agreement with Planck 2018 cosmological constraints.

VI. CONCLUSIONS

In this work we have considered \mathcal{R}^2 theories in the framework of the Palatini formulation. Although this is not new, we have presented a general setup within which inflation models can be studied. The actions, in the Einstein frame, resemble K - inflation models, however additional terms, that are quartic in the derivatives of the fields involved, emerge. For the models studied in this work, these are small during inflation, in accord with the findings of other authors, as we have verified by our numerical approach, which duly takes into account these terms. However, their role towards the end of inflation is essential for the determination of the instantaneous reheating temperature.

This formulation is model independent and can be applied to any inflationary model. These theories are described by three arbitrary functions. Two of them are associated with the coupling of the scalars to the linear and the quadratic terms, with respect the Palatini curvature \mathcal{R} , and the third is a scalar potential. Inflation can be studied in this framework without the need of using canonically normalized fields.

We have applied this for the study of popular inflationary models that are minimally coupled to gravity, with monomial potentials of the form $V \sim h^n$, with the power n a positive and even integer. We also considered the Higgs potential non-minimally coupled to gravity. These models have been put under scrutiny over the years, in the metric formalism, and recently have been extensively studied in the non-metric, or Palatini, formalism. However the stringent constraints arising from the scalar power spectrum measurements have not been duly taken into account, in most of the studies, in conjunction with the reheating temperature of the Universe. In [38] such a study has been undertaken, in the context of the quartic Higgs model that is minimally coupled to gravity.

In this work, without invoking any particular reheating temperature mechanism, we have undertaken

this study, and show that the measurements of the primordial power spectrum amplitude imposes very stringent constraints. These, in combination with the restrictions arising from the measurements of other cosmological observables, in particular the primordial tilt n_s and the tensor to scalar ratio r , restrict considerably these models.

For the quadratic model $V = \frac{m^2}{2}h^2$ we have seen that the scalar power spectrum amplitude A_s puts constraints on the parameter m , and agreement with data is obtained for values of it that lie in a tight range. The maximum reheating, or instantaneous, temperature T_{ins} , is of order $\sim 10^{15} GeV$, and this is attained for fine-tuned values of m , within this range. For these fine-tuned values, the range of the allowed temperatures is rather narrow, and depends on the effective equation of state parameter w , with a lowest temperature not far from the instantaneous temperature. For the canonical scenario, although smaller, this is of the same order of magnitude with T_{ins} . If we allow for small deviations, from this fine-tuned values, agreement with data is still feasible. However these deviations, although they do not disturb substantially the observable n_s , should lie in a narrow range, outside which agreement with A_s data is hard to achieve. In these cases the allowed temperatures are well below T_{ins} and rapid thermalization is not possible. Besides, depending on the value of m , not any value of w in the range $-1/3 < w < 1$ is allowed. The conclusion, concerning this model, is that, agreement with all cosmological data is possible for values of the potential coupling m that lie in a narrow range. Instantaneous reheating is possible at the cost of a very fine-tuned values of m .

The model with the quartic potential $V \sim h^4$ is in conflict with the spectral index n_s data. Only marginal agreement with the primordial tilt can be obtained, with $n_s \simeq 0.960$, but this occurs for very low reheating temperatures close to Nucleosynthesis $T_{reh} \sim MeV$, and for values w close to $w = 1.0$. On the other hand, the amplitude A_s prefers smaller values of the equation of state parameter $w \lesssim 0.25$. The conclusion is that, this model is hard to reconcile with n_s , the scalar power spectrum measurements and reheating temperatures that are reasonably larger than $T_{reh} \sim MeV$ so that we do not run into problems with Big Bang Nucleosynthesis. As our qualitative arguments have shown, for the descendant models, $V \sim h^n$ with $n > 4$, the situation is even worse.

The situation with the quartic potential is rescued in the Higgs model when the scalar field couples in a non-minimal manner to gravity, specified by a parameter ξ . This helps in that, as we have explicitly shown, the value of n_s depends on ξ allowing for larger values of n_s . Agreement with n_s observations demands that ξ is not smaller than about ~ 0.06 . Given ξ , the primordial spectrum measurements in the Higgs model restricts severely the quartic coupling λ . The larger the value of ξ is the largest the values of the allowed λ are. The quartic coupling is small, smaller than $\sim 10^{-6}$, for values ξ that do not exceed $\sim 10^4$. Higher λ values are in principle allowed but these require very large values of ξ leading to instantaneous reheating temperatures, lower than $\sim 10^{15} GeV$. Note that in the Higgs case there is no bound on the parameter a specifying the coupling of the scalar field to the gravity term \mathcal{R}^2 , which, unlike the previous models is unrestricted. Thus both large and low values of a are allowed. Due to that, and for given ξ and λ in the appropriate range, two regimes can be distinguished. The small- a , when $a < \xi^2/\lambda$, and the large $a > \xi^2/\lambda$ regime. In the small a -regime, and particularly when $a \ll \xi^2/\lambda$, the predictions are independent of the parameter a , provided that a stays much smaller than ξ^2/λ . The inflationary scale in this case is $\mu \sim \sqrt{(\lambda/\xi^2)}$ and lies in the range $10^{-5} - 10^{-7}$ Planck masses, for ξ between 0.06 and 10^2 . The instantaneous reheating temperature T_{ins} , in this case, is larger for smaller values of the parameter ξ and receives its largest possible value, $\simeq 2.1 \times 10^{15} GeV$, when ξ is in the vicinity of $\xi \simeq 0.1$.

In the large- a regime, on the other hand, the inflationary scale is $\mu \sim a^{-1/2}$. At the same time T_{ins} behaves as $\sim a^{-1/4}$. Unless a is not exceedingly large, T_{ins} can be as large as $\simeq 10^{15} GeV$, and this requires values of ξ of order unity or so. In both regimes there are values of the parameters for which all cosmological data can be satisfied. However for given ξ , as in the models discussed previously, the quartic coupling λ should lie in a tight range, as the power spectrum observations dictate. Moreover for instantaneous reheating λ should be fine-tuned. In that case the allowed temperatures are close to T_{ins} for the canonical scenario, $w = 0.0$, while a broader range of T_{reh} is allowed, bracketing values $T_{reh} \sim 10^9 GeV$ or so, for values of the equation of state parameter w in the vicinity of $\simeq 0.25$.

Acknowledgments A.B.L. wishes to thank V. C. Spanos and K. Tamvakis for discussions. I.D.G. thanks A. Karam for illuminating discussions. "This research is co-financed by Greece and the European Union (European Social Fund- ESF) through the Operational Programme 'Human Resources Develop-

ment, Education and Lifelong Learning’ in the context of the project ‘Strengthening Human Resources Research Potential via Doctorate Research’ (MIS-5000432), implemented by the State Scholarships Foundation (IKY).”

-
- [1] T. P. Sotiriou, “f(R) gravity and scalar-tensor theory,” *Class. Quant. Grav.* **23**, 5117 (2006), [[gr-qc/0604028](#)].
 - [2] T. P. Sotiriou and S. Liberati, “Metric-affine f(R) theories of gravity,” *Annals Phys.* **322**, 935 (2007), [[gr-qc/0604006](#)].
 - [3] T. P. Sotiriou and V. Faraoni, “f(R) Theories of Gravity,” *Rev. Mod. Phys.* **82**, 451 (2010), [arXiv:0805.1726 \[gr-qc\]](#).
 - [4] M. Borunda, B. Janssen and M. Bastero-Gil, “Palatini versus metric formulation in higher curvature gravity,” *JCAP* **0811**, 008 (2008), [arXiv:0804.4440 \[hep-th\]](#).
 - [5] A. De Felice and S. Tsujikawa, “f(R) theories,” *Living Rev. Rel.* **13**, 3 (2010), [arXiv:1002.4928 \[gr-qc\]](#).
 - [6] G. J. Olmo, “Palatini Approach to Modified Gravity: f(R) Theories and Beyond,” *Int. J. Mod. Phys. D* **20**, 413 (2011), [arXiv:1101.3864 \[gr-qc\]](#).
 - [7] S. Capozziello and M. De Laurentis, “Extended Theories of Gravity,” *Phys. Rept.* **509**, 167 (2011), [arXiv:1108.6266 \[gr-qc\]](#).
 - [8] T. Clifton, P. G. Ferreira, A. Padilla and C. Skordis, “Modified Gravity and Cosmology,” *Phys. Rept.* **513**, 1 (2012), [arXiv:1106.2476 \[astro-ph.CO\]](#).
 - [9] S. Nojiri, S. D. Odintsov and V. K. Oikonomou, “Modified Gravity Theories on a Nutshell: Inflation, Bounce and Late-time Evolution,” *Phys. Rept.* **692**, 1 (2017), [arXiv:1705.11098 \[gr-qc\]](#).
 - [10] A. A. Starobinsky, “A New Type of Isotropic Cosmological Models Without Singularity,” *Phys. Lett.* **91B**, 99 (1980) [*Adv. Ser. Astrophys. Cosmol.* **3**, 130 (1987)].
 - [11] V. F. Mukhanov and G. V. Chibisov, “Quantum Fluctuations and a Nonsingular Universe,” *JETP Lett.* **33**, 532 (1981) [*Pisma Zh. Eksp. Teor. Fiz.* **33**, 549 (1981)].
 - [12] A. A. Starobinsky, “The Perturbation Spectrum Evolving from a Nonsingular Initially De-Sitter Cosmology and the Microwave Background Anisotropy,” *Sov. Astron. Lett.* **9**, 302 (1983).
 - [13] F. Bauer and D. A. Demir, “Inflation with Non-Minimal Coupling: Metric versus Palatini Formulations,” *Phys. Lett. B* **665**, 222 (2008), [arXiv:0803.2664 \[hep-ph\]](#).
 - [14] T. Koivisto and H. Kurki-Suonio, “Cosmological perturbations in the palatini formulation of modified gravity,” *Class. Quant. Grav.* **23**, 2355 (2006), [[astro-ph/0509422](#)].
 - [15] N. Tamanini and C. R. Contaldi, “Inflationary Perturbations in Palatini Generalised Gravity,” *Phys. Rev. D* **83**, 044018 (2011), [arXiv:1010.0689 \[gr-qc\]](#).
 - [16] F. Bauer and D. A. Demir, “Higgs-Palatini Inflation and Unitarity,” *Phys. Lett. B* **698**, 425 (2011), [arXiv:1012.2900 \[hep-ph\]](#).
 - [17] K. Enqvist, T. Koivisto and G. Rigopoulos, “Non-metric chaotic inflation,” *JCAP* **1205**, 023 (2012), [arXiv:1107.3739, \[astro-ph.CO\]](#).
 - [18] A. Borowiec, M. Kamionka, A. Kurek and M. Szydlowski, “Cosmic acceleration from modified gravity with Palatini formalism,” *JCAP* **1202**, 027 (2012), [arXiv:1109.3420 \[gr-qc\]](#).
 - [19] A. Stachowski, M. Szydlowski and A. Borowiec, “Starobinsky cosmological model in Palatini formalism,” *Eur. Phys. J. C* **77**, no. 6, 406 (2017), [arXiv:1608.03196 \[gr-qc\]](#).
 - [20] C. Fu, P. Wu and H. Yu, “Inflationary dynamics and preheating of the nonminimally coupled inflaton field in the metric and Palatini formalisms,” *Phys. Rev. D* **96**, no. 10, 103542 (2017), [arXiv:1801.04089 \[gr-qc\]](#).
 - [21] S. Rasanen and P. Wahlman, “Higgs inflation with loop corrections in the Palatini formulation,” *JCAP* **1711**, no. 11, 047 (2017), [arXiv:1709.07853 \[astro-ph.CO\]](#).
 - [22] T. Tenkanen, “Resurrecting Quadratic Inflation with a non-minimal coupling to gravity,” *JCAP* **1712**, no. 12, 001 (2017), [arXiv:1710.02758 \[astro-ph.CO\]](#).
 - [23] A. Racioppi, “Coleman-Weinberg linear inflation: metric vs. Palatini formulation,” *JCAP* **1712**, no. 12, 041 (2017), [arXiv:1710.04853 \[astro-ph.CO\]](#).
 - [24] T. Markkanen, T. Tenkanen, V. Vaskonen and H. Veermäe, “Quantum corrections to quartic inflation with a non-minimal coupling: metric vs. Palatini,” *JCAP* **1803**, no. 03, 029 (2018), [arXiv:1712.04874 \[gr-qc\]](#).
 - [25] L. Järv, A. Racioppi and T. Tenkanen, “Palatini side of inflationary attractors,” *Phys. Rev. D* **97**, no. 8, 083513 (2018), [arXiv:1712.08471 \[gr-qc\]](#).
 - [26] S. Rasanen, “Higgs inflation in the Palatini formulation with kinetic terms for the metric,” *The Open Journal of Astrophysics*, 2018, [arXiv:1811.09514 \[gr-qc\]](#).
 - [27] A. Racioppi, “New universal attractor in nonminimally coupled gravity: Linear inflation,” *Phys. Rev. D* **97**, no. 12, 123514 (2018), [arXiv:1801.08810 \[astro-ph.CO\]](#).

- [28] P. Carrilho, D. Mulryne, J. Ronayne and T. Tenkanen, “Attractor Behaviour in Multifield Inflation,” *JCAP* **1806**, no. 06, 032 (2018), [arXiv:1804.10489 \[astro-ph.CO\]](#).
- [29] V. M. Enckell, K. Enqvist, S. Rasanen and E. Tomberg, “Higgs inflation at the hilltop,” *JCAP* **1806**, no. 06, 005 (2018), [arXiv:1802.09299 \[astro-ph.CO\]](#).
- [30] F. Bombacigno and G. Montani, “Big bounce cosmology for Palatini R^2 gravity with a Nieh-Yan term,” *Eur. Phys. J. C* **79**, no. 5, 405 (2019), [arXiv:1809.07563 \[gr-qc\]](#).
- [31] V. M. Enckell, K. Enqvist, S. Rasanen and L. P. Wahlman, “Inflation with R^2 term in the Palatini formalism,” *JCAP* **1902**, 022 (2019), [arXiv:1810.05536 \[gr-qc\]](#).
- [32] I. Antoniadis, A. Karam, A. Lykkas and K. Tamvakis, “Palatini inflation in models with an R^2 term,” *JCAP* **1811**, 028 (2018), [arXiv:1810.10418 \[gr-qc\]](#).
- [33] I. Antoniadis, A. Karam, A. Lykkas, T. Pappas and K. Tamvakis, “Rescuing Quartic and Natural Inflation in the Palatini Formalism,” *JCAP* **1903**, 005 (2019), [arXiv:1812.00847 \[gr-qc\]](#).
- [34] S. Rasanen and E. Tomberg, “Planck scale black hole dark matter from Higgs inflation,” *JCAP* **1901**, 038 (2019), [arXiv:1810.12608 \[astro-ph.CO\]](#).
- [35] J. P. B. Almeida, N. Bernal, J. Rubio and T. Tenkanen, “Hidden Inflaton Dark Matter,” *JCAP* **1903**, 012 (2019), [arXiv:1811.09640 \[hep-ph\]](#).
- [36] T. Takahashi and T. Tenkanen, “Towards distinguishing variants of non-minimal inflation,” *JCAP* **1904**, no. 04, 035 (2019), [arXiv:1812.08492 \[astro-ph.CO\]](#).
- [37] K. Kannike, A. Kubarski, L. Marzola and A. Racioppi, “A minimal model of inflation and dark radiation,” *Phys. Lett. B* **792**, 74 (2019), [arXiv:1810.12689 \[hep-ph\]](#).
- [38] T. Tenkanen, “Minimal Higgs inflation with an R^2 term in Palatini gravity,” *Phys. Rev. D* **99**, no. 6, 063528 (2019), [arXiv:1901.01794 \[astro-ph.CO\]](#).
- [39] K. Shimada, K. Aoki and K. i. Maeda, “Metric-affine Gravity and Inflation,” *Phys. Rev. D* **99**, no. 10, 104020 (2019), [arXiv:1812.03420 \[gr-qc\]](#).
- [40] J. Wu, G. Li, T. Harko and S. D. Liang, “Palatini formulation of $f(R, T)$ gravity theory, and its cosmological implications,” *Eur. Phys. J. C* **78**, no. 5, 430 (2018), [arXiv:1805.07419 \[gr-qc\]](#).
- [41] A. Kozak and A. Borowiec, “Palatini frames in scalar tensor theories of gravity,” *Eur. Phys. J. C* **79**, no. 4, 335 (2019), [arXiv:1808.05598 \[hep-th\]](#).
- [42] R. Jinno, K. Kaneta, K. y. Oda and S. C. Park, “Hillclimbing inflation in metric and Palatini formulations,” *Phys. Lett. B* **791**, 396 (2019), [arXiv:1812.11077 \[gr-qc\]](#).
- [43] A. Edery and Y. Nakayama, “Palatini formulation of pure R^2 gravity yields Einstein gravity with no massless scalar,” *Phys. Rev. D* **99**, no. 12, 124018 (2019), [arXiv:1902.07876 \[hep-th\]](#).
- [44] J. Rubio and E. S. Tomberg, “Preheating in Palatini Higgs inflation,” *JCAP* **1904**, 021 (2019), [arXiv:1902.10148 \[hep-ph\]](#).
- [45] R. Jinno, M. Kubota, K. y. Oda and S. C. Park, “Higgs inflation in metric and Palatini formalisms: Required suppression of higher dimensional operators,” [arXiv:1904.05699 \[hep-ph\]](#).
- [46] M. Giovannini, “Post-inflationary phases stiffer than radiation and Palatini formulation,” [arXiv:1905.06182 \[gr-qc\]](#).
- [47] T. Tenkanen and L. Visinelli, “Axion dark matter from Higgs inflation with an intermediate H_* ,” *JCAP* **1908**, 033 (2019), [arXiv:1906.11837 \[astro-ph.CO\]](#).
- [48] N. Bostan, “Quadratic, Higgs and hilltop potentials in the Palatini gravity,” [arXiv:1908.09674 \[astro-ph.CO\]](#).
- [49] T. Tenkanen, “Trans-Planckian Censorship, Inflation and Dark Matter,” [arXiv:1910.00521 \[astro-ph.CO\]](#).
- [50] N. Aghanim *et al.* [Planck Collaboration], “Planck 2018 results. VI. Cosmological parameters,” [arXiv:1807.06209 \[astro-ph.CO\]](#).
- [51] Y. Akrami *et al.* [Planck Collaboration], “Planck 2018 results. X. Constraints on inflation,” [arXiv:1807.06211v2 \[astro-ph.CO\]](#).
- [52] P. A. R. Ade *et al.* [BICEP2 and Keck Array Collaborations], “BICEP2 / Keck Array x: Constraints on Primordial Gravitational Waves using Planck, WMAP, and New BICEP2/Keck Observations through the 2015 Season,” *Phys. Rev. Lett.* **121**, 221301 (2018), [arXiv:1810.05216 \[astro-ph.CO\]](#).
- [53] M. Gerbino, K. Freese, S. Vagnozzi, M. Lattanzi, O. Mena, E. Giusarma and S. Ho, “Impact of neutrino properties on the estimation of inflationary parameters from current and future observations,” *Phys. Rev. D* **95** (2017) no.4, 043512, [arXiv:1610.08830 \[astro-ph.CO\]](#).
- [54] C. Armendariz-Picon, T. Damour and V. F. Mukhanov, “k - inflation,” *Phys. Lett. B* **458**, 209 (1999), [[hep-th/9904075](#)].
- [55] J. Garriga and V. F. Mukhanov, “Perturbations in k-inflation,” *Phys. Lett. B* **458**, 219 (1999), [[hep-th/9904176](#)].
- [56] L. Lorenz, J. Martin and C. Ringeval, “Constraints on Kinetically Modified Inflation from WMAP5,” *Phys. Rev. D* **78**, 063543 (2008), [[arXiv:0807.2414 \[astro-ph\]](#)].
- [57] S. Li and A. R. Liddle, “Observational constraints on K-inflation models,” *JCAP* **1210**, 011 (2012),

- arXiv:1204.6214 [astro-ph.CO].
- [58] A. A. Starobinsky, “Spectrum of relict gravitational radiation and the early state of the universe,” *JETP Lett.* **30**, 682 (1979) [*Pisma Zh. Eksp. Teor. Fiz.* **30**, 719 (1979)].
 - [59] V. F. Mukhanov, “Gravitational Instability of the Universe Filled with a Scalar Field,” *JETP Lett.* **41**, 493 (1985) [*Pisma Zh. Eksp. Teor. Fiz.* **41**, 402 (1985)].
 - [60] V. F. Mukhanov, *Sov. Phys. JETP* **67**, 1297 (1988) [*Zh. Eksp. Teor. Fiz.* **94N7**, 1 (1988)].
 - [61] F. Lucchin and S. Matarrese, “Power Law Inflation,” *Phys. Rev. D* **32**, 1316 (1985).
 - [62] E. D. Stewart and D. H. Lyth, “A More accurate analytic calculation of the spectrum of cosmological perturbations produced during inflation,” *Phys. Lett. B* **302**, 171 (1993), [gr-qc/9302019].
 - [63] J. O. Gong and E. D. Stewart, “The Density perturbation power spectrum to second order corrections in the slow roll expansion,” *Phys. Lett. B* **510**, 1 (2001), [astro-ph/0101225].
 - [64] D. J. Schwarz, C. A. Terrero-Escalante and A. A. Garcia, “Higher order corrections to primordial spectra from cosmological inflation,” *Phys. Lett. B* **517**, 243 (2001), [astro-ph/0106020].
 - [65] S. M. Leach, A. R. Liddle, J. Martin and D. J. Schwarz, “Cosmological parameter estimation and the inflationary cosmology,” *Phys. Rev. D* **66**, 023515 (2002), [astro-ph/0202094].
 - [66] S. Habib, K. Heitmann, G. Jungman and C. Molina-Paris, “The Inflationary perturbation spectrum,” *Phys. Rev. Lett.* **89**, 281301 (2002), [astro-ph/0208443].
 - [67] J. Martin and D. J. Schwarz, “WKB approximation for inflationary cosmological perturbations,” *Phys. Rev. D* **67**, 083512 (2003), [astro-ph/0210090].
 - [68] S. Habib, A. Heinen, K. Heitmann, G. Jungman and C. Molina-Paris, “Characterizing inflationary perturbations: The Uniform approximation,” *Phys. Rev. D* **70**, 083507 (2004), [astro-ph/0406134].
 - [69] H. Wei, R. G. Cai and A. Wang, “Second-order corrections to the power spectrum in the slow-roll expansion with a time-dependent sound speed,” *Phys. Lett. B* **603**, 95 (2004), [hep-th/0409130].
 - [70] R. Casadio, F. Finelli, M. Luzzi and G. Venturi, “Improved WKB analysis of cosmological perturbations,” *Phys. Rev. D* **71**, 043517 (2005), [gr-qc/0410092].
 - [71] R. Casadio, F. Finelli, M. Luzzi and G. Venturi, “Higher order slow-roll predictions for inflation,” *Phys. Lett. B* **625**, 1 (2005), [gr-qc/0506043].
 - [72] W. H. Kinney and K. Tzirakis, “Quantum modes in DBI inflation: exact solutions and constraints from vacuum selection,” *Phys. Rev. D* **77**, 103517 (2008), [arXiv:0712.2043 [astro-ph]].
 - [73] L. Lorenz, J. Martin and C. Ringeval, “K-inflationary Power Spectra in the Uniform Approximation,” *Phys. Rev. D* **78**, 083513 (2008), [arXiv:0807.3037 [astro-ph]].
 - [74] N. Agarwal and R. Bean, “Cosmological constraints on general, single field inflation,” *Phys. Rev. D* **79**, 023503 (2009), [arXiv:0809.2798 [astro-ph]].
 - [75] J. Martin, C. Ringeval and V. Vennin, “K-inflationary Power Spectra at Second Order,” *JCAP* **1306**, 021 (2013), [arXiv:1303.2120 [astro-ph.CO]].
 - [76] J. Beltran Jimenez, M. Musso and C. Ringeval, “Exact Mapping between Tensor and Most General Scalar Power Spectra,” *Phys. Rev. D* **88**, 043524 (2013), [arXiv:1303.2788 [astro-ph.CO]].
 - [77] A. L. Alinea, T. Kubota and W. Naylor, “Logarithmic divergences in the k -inflationary power spectra computed through the uniform approximation,” *JCAP* **1602**, 028 (2016), [arXiv:1506.08344 [gr-qc]].
 - [78] A. R. Liddle and S. M. Leach, “How long before the end of inflation were observable perturbations produced?,” *Phys. Rev. D* **68**, 103503 (2003), [astro-ph/0305263].
 - [79] S. Dodelson and L. Hui, “A Horizon ratio bound for inflationary fluctuations,” *Phys. Rev. Lett.* **91**, 131301 (2003), [astro-ph/0305113].
 - [80] J. Martin and C. Ringeval, “First CMB Constraints on the Inflationary Reheating Temperature,” *Phys. Rev. D* **82**, 023511 (2010), arXiv:1004.5525 [astro-ph.CO].
 - [81] K. D. Lozanov and M. A. Amin, “Self-resonance after inflation: oscillons, transients and radiation domination,” *Phys. Rev. D* **97**, no. 2, 023533 (2018), arXiv:1710.06851 [astro-ph.CO].
 - [82] R. Allahverdi, R. Brandenberger, F. Y. Cyr-Racine and A. Mazumdar, “Reheating in Inflationary Cosmology: Theory and Applications,” *Ann. Rev. Nucl. Part. Sci.* **60**, 27 (2010), arXiv:1001.2600 [hep-th].
 - [83] D. I. Podolsky, G. N. Felder, L. Kofman and M. Peloso, “Equation of state and beginning of thermalization after preheating,” *Phys. Rev. D* **73**, 023501 (2006), [hep-ph/0507096].
 - [84] P. Adshead, R. Easther, J. Pritchard and A. Loeb, “Inflation and the Scale Dependent Spectral Index: Prospects and Strategies,” *JCAP* **1102**, 021 (2011), arXiv:1007.3748 [astro-ph.CO].
 - [85] J. Mielczarek, “Reheating temperature from the CMB,” *Phys. Rev. D* **83**, 023502 (2011), arXiv:1009.2359 [astro-ph.CO].
 - [86] R. Easther and H. V. Peiris, “Bayesian Analysis of Inflation II: Model Selection and Constraints on Reheating,” *Phys. Rev. D* **85**, 103533 (2012), arXiv:1112.0326 [astro-ph.CO].
 - [87] L. Dai, M. Kamionkowski and J. Wang, “Reheating constraints to inflationary models,” *Phys. Rev. Lett.*

- 113**, 041302 (2014), [arXiv:1404.6704 \[astro-ph.CO\]](#).
- [88] J. B. Munoz and M. Kamionkowski, “Equation-of-State Parameter for Reheating,” *Phys. Rev. D* **91**, no. 4, 043521 (2015), [arXiv:1412.0656 \[astro-ph.CO\]](#).
- [89] J. L. Cook, E. Dimastrogiovanni, D. A. Easson and L. M. Krauss, “Reheating predictions in single field inflation,” *JCAP* **1504**, 047 (2015), [arXiv:1502.04673 \[astro-ph.CO\]](#).
- [90] J. O. Gong, S. Pi and G. Leung, “Probing reheating with primordial spectrum,” *JCAP* **1505**, 027 (2015), [arXiv:1501.03604 \[hep-ph\]](#).
- [91] T. Rehagen and G. B. Gelmini, “Low reheating temperatures in monomial and binomial inflationary potentials,” *JCAP* **1506**, 039 (2015), [arXiv:1504.03768 \[hep-ph\]](#).
- [92] K. D. Lozanov and M. A. Amin, “Equation of State and Duration to Radiation Domination after Inflation,” *Phys. Rev. Lett.* **119**, no. 6, 061301 (2017), [arXiv:1608.01213 \[astro-ph.CO\]](#).
- [93] M. Kawasaki, K. Kohri and N. Sugiyama, “Cosmological constraints on late time entropy production,” *Phys. Rev. Lett.* **82** (1999) 4168, [astro-ph/9811437](#).
- [94] T. Hasegawa, N. Hiroshima, K. Kohri, R. S. L. Hansen, T. Tram and S. Hannestad, “MeV-scale reheating temperature and thermalization of oscillating neutrinos by radiative and hadronic decays of massive particles,” [arXiv:1908.10189 \[hep-ph\]](#).
- [95] J. J. M. Carrasco, R. Kallosh and A. Linde, “Cosmological Attractors and Initial Conditions for Inflation,” *Phys. Rev. D* **92**, no. 6, 063519 (2015), [arXiv:1506.00936 \[hep-th\]](#), [cea-01690086](#).
- [96] F. L. Bezrukov and M. Shaposhnikov, “The Standard Model Higgs boson as the inflaton,” *Phys. Lett. B* **659**, 703 (2008), [arXiv:0710.3755 \[hep-th\]](#).
- [97] F. L. Bezrukov, A. Magnin and M. Shaposhnikov, “Standard Model Higgs boson mass from inflation,” *Phys. Lett. B* **675**, 88 (2009), [arXiv:0812.4950 \[hep-ph\]](#).
- [98] J. L. F. Barbon and J. R. Espinosa, “On the Naturalness of Higgs Inflation,” *Phys. Rev. D* **79**, 081302 (2009), [arXiv:0903.0355 \[hep-ph\]](#).
- [99] A. O. Barvinsky, A. Y. Kamenshchik, C. Kiefer, A. A. Starobinsky and C. Steinwachs, “Asymptotic freedom in inflationary cosmology with a non-minimally coupled Higgs field,” *JCAP* **0912**, 003 (2009), [arXiv:0904.1698 \[hep-ph\]](#).
- [100] A. O. Barvinsky, A. Y. Kamenshchik, C. Kiefer, A. A. Starobinsky and C. F. Steinwachs, “Higgs boson, renormalization group, and naturalness in cosmology,” *Eur. Phys. J. C* **72**, 2219 (2012), [arXiv:0910.1041 \[hep-ph\]](#).
- [101] C. Germani and A. Kehagias, “New Model of Inflation with Non-minimal Derivative Coupling of Standard Model Higgs Boson to Gravity,” *Phys. Rev. Lett.* **105**, 011302 (2010), [arXiv:1003.2635 \[hep-ph\]](#).
- [102] C. Germani and A. Kehagias, “Cosmological Perturbations in the New Higgs Inflation,” *JCAP* **1005**, 019 (2010), Erratum: [*JCAP* **1006**, E01 (2010)], [arXiv:1003.4285 \[astro-ph.CO\]](#).
- [103] R. N. Lerner and J. McDonald, “A Unitarity-Conserving Higgs Inflation Model,” *Phys. Rev. D* **82**, 103525 (2010), [arXiv:1005.2978 \[hep-ph\]](#).
- [104] F. Bezrukov, A. Magnin, M. Shaposhnikov and S. Sibiryakov, “Higgs inflation: consistency and generalisations,” *JHEP* **1101**, 016 (2011), [arXiv:1008.5157 \[hep-ph\]](#).
- [105] K. Kamada, T. Kobayashi, M. Yamaguchi and J. Yokoyama, “Higgs G-inflation,” *Phys. Rev. D* **83**, 083515 (2011), [arXiv:1012.4238 \[astro-ph.CO\]](#).
- [106] K. Kamada, T. Kobayashi, T. Takahashi, M. Yamaguchi and J. Yokoyama, “Generalized Higgs inflation,” *Phys. Rev. D* **86**, 023504 (2012), [arXiv:1203.4059 \[hep-ph\]](#).
- [107] F. Bezrukov, “The Higgs field as an inflaton,” *Class. Quant. Grav.* **30**, 214001 (2013), [arXiv:1307.0708 \[hep-ph\]](#).
- [108] K. Allison, “Higgs xi-inflation for the 125-126 GeV Higgs: a two-loop analysis,” *JHEP* **1402**, 040 (2014), [arXiv:1306.6931 \[hep-ph\]](#).
- [109] F. Bezrukov and M. Shaposhnikov, “Higgs inflation at the critical point,” *Phys. Lett. B* **734**, 249 (2014), [arXiv:1403.6078 \[hep-ph\]](#).
- [110] Y. Hamada, H. Kawai, K. y. Oda and S. C. Park, “Higgs inflation from Standard Model criticality,” *Phys. Rev. D* **91**, 053008 (2015), [arXiv:1408.4864 \[hep-ph\]](#).
- [111] A. Salvio and A. Mazumdar, “Classical and Quantum Initial Conditions for Higgs Inflation,” *Phys. Lett. B* **750**, 194 (2015), [arXiv:1506.07520 \[hep-ph\]](#).
- [112] X. Calmet and I. Kuntz, “Higgs Starobinsky Inflation,” *Eur. Phys. J. C* **76**, no. 5, 289 (2016), [arXiv:1605.02236 \[hep-th\]](#).
- [113] R. Jinno, K. Kaneta and K. y. Oda, “Hill-climbing Higgs inflation,” *Phys. Rev. D* **97**, no. 2, 023523 (2018), [arXiv:1705.03696 \[hep-ph\]](#).
- [114] F. Bezrukov, M. Pauly and J. Rubio, “On the robustness of the primordial power spectrum in renormalized Higgs inflation,” *JCAP* **1802**, 040 (2018), [arXiv:1706.05007 \[hep-ph\]](#).
- [115] M. He, A. A. Starobinsky and J. Yokoyama, “Inflation in the mixed Higgs- R^2 model,” *JCAP* **1805**, 064

- (2018), [arXiv:1804.00409](#) [astro-ph.CO].
- [116] A. Gundhi and C. F. Steinwachs, “Scalaron-Higgs inflation,” [arXiv:1810.10546](#) [hep-th].
 - [117] J. Rubio, “Higgs inflation,” [Front. Astron. Space Sci.](#) **5**, 50 (2019), [arXiv:1807.02376](#) [hep-ph].
 - [118] M. He, R. Jinno, K. Kamada, S. C. Park, A. A. Starobinsky and J. Yokoyama, “On the violent preheating in the mixed Higgs- R^2 inflationary model,” [Phys. Lett. B](#) **791**, 36 (2019) , [arXiv:1812.10099](#) [hep-ph].
 - [119] C. F. Steinwachs, “Higgs field in cosmology,” [arXiv:1909.10528](#) [hep-ph].